



Published in final edited form as:

Eur J Med Chem. 2012 January ; 47(1): 432–444. doi:10.1016/j.ejmech.2011.11.012.

From COX-2 inhibitor nimesulide to potent anti-cancer agent: synthesis, *in vitro*, *in vivo* and pharmacokinetic evaluation

Bo Zhong^{#a}, Xiaohan Cai^{#a}, Snigdha Chennamaneni^a, Xin Yi^a, lili Liu^c, John J. Pink^d, Afshin Dowlati^c, Yan Xu^a, Aimin Zhou^{a,b}, and Bin Su^{a,b,*}

^aDepartment of Chemistry, College of Sciences and Health Professions, Cleveland State University, 2121 Euclid Ave., Cleveland, OH, 44115, USA

^bCenter for Gene Regulation in Health and Disease, College of Sciences & Health Professions, Cleveland State University, 2121 Euclid Ave., Cleveland, OH, 44115, USA

^cDivision of Hematology and Oncology, Case Western Reserve University School of Medicine, 10900 Euclid Avenue, Cleveland, OH 44106, USA

^dDivision of General Medical Sciences-Oncology, Case Western Reserve University School of Medicine, 10900 Euclid Avenue, Cleveland, OH 44106, USA

These authors contributed equally to this work.

Abstract

Cyclooxygenase-2 (COX-2) inhibitor nimesulide inhibits the proliferation of various types of cancer cells mainly via COX-2 independent mechanisms, which makes it a good lead compound for anti-cancer drug development. In the presented study, a series of new nimesulide analogs were synthesized based on the structure–function analysis generated previously. Some of them displayed very potent anti-cancer activity with IC₅₀s around 100nM to 200nM to inhibit SKBR-3 breast cancer cell growth. CSUOH0901 (NSC751382) from the compound library also inhibits the growth of the 60 cancer cell lines used at National Cancer Institute Developmental therapeutics Program (NCIDTP) with IC₅₀s around 100nM to 500nM. Intraperitoneal injection with a dosage of 5mg/kg/d of CSUOH0901 to nude mice suppresses HT29 colorectal xenograft growth. Pharmacokinetic studies demonstrate the good bioavailability of the compound.

Keywords

COX-2 inhibitor; nimesulide; anti-cancer; xenograft; pharmacokinetics

*To whom correspondence should be addressed: Bin Su, Ph.D., Department of Chemistry, College of Sciences and Health Professions, Cleveland State University, 2121 Euclid Ave., Cleveland, OH 44115, USA, Phone: 216-687-9219, Fax: 216-687-9298, B.su@csuohio.edu.

Supporting Information Available

HPLC Analysis for compounds 1-39; the dose-dependent results of CSUOH0901(NSC751382) on the growth inhibition of 60 cancer cell lines.

1. Introduction

Numerous studies have demonstrated the overexpression of cyclooxygenase-2 (COX-2) in solid malignancies [1-9]. Epidemiological, clinical, and preclinical investigations also provide compelling evidence that COX-2 inhibitors could act as chemopreventive agents [8,10-12]. The anti-cancer effects of COX-2 inhibitors are based on the assumption that prostaglandins generated by COX-2 promote tumor growth in an autocrine and/or paracrine manner [13,14].

Theoretically, COX-2 inhibitors exhibit all the anti-cancer or cancer preventive activity by blocking COX-2, thereby decrease the concentration of prostaglandins inside the tumor. However, these small molecules may also target other growth pathway, which may lead to cell growth inhibition, apoptosis or necrosis [8,15,16]. Many COX-2 inhibitors can suppress the growth of non-COX-2 expressing tumor cells, while supplementation with exogenous prostaglandin cannot rescue the cells from growth inhibition caused by COX-2 inhibitors [17-22]. Therefore, it is speculated that COX-2-independent effects may contribute to or even be fully responsible for the anti-cancer properties of some COX-2 inhibitors. Furthermore, the relative potency of COX-2 inhibitors to inhibit COX-2 enzyme does not match their potency to inhibit cancer cell growth [19]. In addition to the lack of correlation between COX-2 inhibition and anti-cancer activities, the required concentrations of these COX-2 inhibitors to inhibit tumor cell growth significantly exceed the concentrations required to inhibit COX-2. This phenomenon suggests that the COX-2 inhibitors mainly target other pathways which need much high concentration for COX-2 inhibitors to block [19,23-26]. The strongest evidence for a COX-independent mechanism is that some non-COX-2 inhibitory derivatives of certain COX-2 inhibitors still exhibit significant anti-cancer activity [27,28].

The COX-2 selective inhibitor nimesulide, *N*-(2-phenoxy-4-nitrophenyl)methanesulfonamide, is a promising lead compound for anti-cancer drug discovery. In several *in vivo* experiments, nimesulide exhibits chemopreventive activity against 2-amino-1-methyl-6-phenylimidazo [4,5-*b*] pyridine-induced mammary carcinogenesis in rats and against the post-initiation development of squamous cell carcinomas in 4-nitroquinoline-1-oxide-induced rat tongue carcinogenesis [29-31]. In addition, nimesulide is shown to protect against *N*-nitrosobis(2-oxopropyl)amine-induced pancreatic tumors in hamster [32]. In some *in vitro* experiments, nimesulide is able to inhibit the proliferation and to increase the apoptosis rate of various types of cancer cells [18,25,33-38]. However, the nimesulide concentrations used in these studies are ranged from 200 to 500 μ M, which greatly exceed the concentration necessary to inhibit COX-2 activity. These facts suggest that nimesulide inhibits cancer cell growth and induces cancer cell apoptosis independent of COX-2.

JCC76 is a non-COX-2 active nimesulide analog (Figure 1) [39-41], and it inhibits SKBR-3 breast cancer cell growth with an IC₅₀ of 1.38 μ M, which is about 100 fold more active than nimesulide (Table 1). The N-Methylation of JCC76 blocks the ionization of the sulfonamide group, which abolishes the potential COX-2 activity [42-44]. In addition, the aromatic nitro group is converted to an amide moiety on the structure of JCC76, which could diminish the

potential hepatotoxicity, since nimesulide shows hepatotoxicity due to the multistep nitroreductive bioactivation that produces the hazardous nitroanion radical and nitroso intermediate [45]. Based on the structure of JCC76, more analogs were designed and synthesized in the current studies. Some new analogs such as CSUOH0901 (NSC751382) inhibited SKBR-3 breast cancer cell growth with IC_{50} s around 0.1 μ M to 0.2 μ M, which is about 10 fold more active than JCC76 and almost 1000 fold more active than nimesulide. In addition, CSUOH0901 inhibited the growth of a broad range of cancer cell lines with IC_{50} s of 0.2 μ M to 0.5 μ M. It also inhibited the growth of HT29 colorectal xenograft in nude mice as well. All the studies suggest that the newly developed JCC76 derivatives are promising anti-cancer drug candidates.

2. Results and discussion

2.1. Compound design and parallel synthesis of JCC76 derivatives

In previous studies, systematic modification was performed on the structure of nimesulide to improve the anti-cancer activity and erase the COX-2 inhibitory activity [41,46]. SAR result suggests that the di-methyl benzyl and methylsulfonamide moieties are critical for the nimesulide analogs to inhibit cancer cell growth (Figure 1). Further, the conversion of the nitro group to a bulky amide moiety generated novel anti-cancer agent JCC76 [39-41,46]. In the current study, di-methyl benzyl and methylsulfonamide groups which are important for the anti-cancer activity of the derivatives were maintained, and we focused on the modification of the amide moiety of JCC76. Various chemical structures including alkyl amide groups, electron-donating or withdrawing group substituted benzamides, bulky or small group substituted benzamides, and heterocyclic amides were introduced at this moiety.

The synthesis is described in Scheme 1. The starting material 2-amino-5-nitrophenol was refluxed with K_2CO_3 and 2, 5-dimethyl benzyl chloride to obtain compound **a**. Sodium hydride and methanesulfonyl chloride were added to compound **a** in dry dimethylformamide (DMF) at room temperature and the reaction mixture was stirred at room temperature overnight to obtain the N,N-bimethanesulfonamido **b**. Compound **b** was hydrolyzed with 10% NaOH solution to generate **c** as a monomethanesulfonamido compound. Compound **c** was treated with sodium hydride and methyl iodine in DMF at room temperature to obtain compound **d**. Then the nitro group was reduced to an amine group to obtain compound **e**. Compound **e** was treated with different substituted acetyl chloride and K_2CO_3 to generate the substituted benzamides **1-39**, respectively. Structures of all the synthesized compounds were determined by 1H -NMR, MS, and their purity was confirmed by HPLC with two mobile phases.

2.2. Biological evaluation of the new analogs with breast cancer cell line SKBR-3

The compounds were tested for the inhibition of SKBR-3 breast cancer cell growth (Table 1). Subsequently, a detailed structure activity analysis was performed based on the structure and the anti-cancer activity. The new derivatives have same core structure as JCC76, the different activity is correlated with the different amide moieties.

For the substituted benzamide moiety in the structure, *para* position bulky halogen substituted benzamide such as **9** (bromine) with an IC₅₀ of 0.22 μM and **29** (iodine) with an IC₅₀ of 0.13 μM show better potency than JCC76, whereas small halogen chlorine at *para* position (**28**) slightly decreases the activity with an IC₅₀ of 2.15 μM. It is also possible that the activity is related to the electronegativity or electron density of the halogens. Iodine has the lowest electronegativity and highest electron density, which may contribute to the potent anti-cancer activity. **2**, **8**, **25**, **20**, and **27**, which have single *meta* substitution groups, display weaker inhibitory activity with IC₅₀s ranging from 1.97 μM to 7.34 μM. It seems that single *meta* substitution is predominated by steric effect. The activity is decreased no matter the substitution is electron-donating or withdrawing group. Dual chlorine substitution (**4** and **14**) slightly increases the activity compared to JCC76, with IC₅₀ of 0.91 μM and 0.80 μM respectively. **1**, **2**, **3**, **7**, **8**, **15**, **21** and **34**, which have electron-withdrawing groups as substitution, exhibit IC₅₀s among 1.0 μM to 3.0 μM. The results suggest that electron-withdrawing groups such as nitro, cyano, multi-fluoro, and trifluoro-methyl substituted benzamide do not increase the activity. **26** shows very weaker activity with an IC₅₀ of 55.35 μM, which possibly is due to the very strong electron-withdrawing effect and the *meta* position steric effect of the di-trifluoro-methyl groups. Most of the strong electron-donating groups such as methoxyl and multi-methoxyl substituted benzamide (**10**, **11**, **16**, **18** and **19**) increase the activity with IC₅₀s among 0.19 μM to 0.68 μM. However, *para*-methyl benzamide (**33**) and *para*-ethyl benzamide (**36**) show lesser potency with IC₅₀s of 2.48 μM and 2.82 μM respectively, although both methyl and ethyl groups are electron donating substitution. It suggests that *para* position steric effect reduces the activity, but strong electron-donating group at *para* position overall increase the activity because the electron donating effect overcomes the steric effect. 2-Naphthyl amide (**5**) increases the activity with an IC₅₀ of 0.21 μM, but 1-Naphthyl amide (**25**) decreases the activity with an IC₅₀ of 3.95 μM. Because 2-Naphthyl group is more like a dual *para* and *meta* position substituted benzamide, and the substitution has very strong electron donating effect at *para* position due to the super conjugation effect. 1-Naphthyl group is more like a dual *meta* and *ortho* position substituted benzamide, which decreases the activity due to steric effect of *meta* substitution. **6** (*para*-phenyl benzamide) shows weaker activity with an IC₅₀ of 2.28 μM. Because the phenyl group cannot form super conjugation with the benzamide due to the steric effect of the two phenyl rings. It makes the phenyl substitution predominated mainly by steric effect. Substituted Benzylamide, namely **17** and **24**, display much weaker activity with IC₅₀s above 30 μM. Heterocyclic amides (**37**, **38**, **39**) decrease the activity, with IC₅₀s of 16.65 μM, 20.12 μM, and 21.88 μM respectively. The results suggest that benzamide moiety is better for the activity compared to the heterocyclic amides.

For the alkyl-substituted amide, lead compound JCC76 is still the most potent one with an IC₅₀ of 1.38 μM. Small alkyl groups such as ethyl (**12**), 3-pentyl (**22**), and cyclopentyl(**23**) greatly decrease the activity, and the corresponding IC₅₀ are 43.27 μM, 51.24 μM, and 11.21 μM respectively. Very bulky alkyl group such as hexadecanyl (**13**) decreases the activity as well, with an IC₅₀ of 11.05 μM. It appears that the best alkyl substitution is a middle size and closed ring.

Overall, *para* position of the benzamide is very critical for the anti-cancer activity of the JCC76 analogs. Strong electron-donating groups at *para* position significantly increase the activity. Single *meta* substituted benzamide greatly decreases the activity, no matter it is electron-donating or withdrawing group as substitution. Several very potent analogs (**5**, **9**, **10**, **16**, **18**, **29**), which are about 5 to 10 fold more active than JCC76, share some structure similarity: *para* position substituted benzamide, or *para* and *meta* both electron-donating group substituted benzamide. **10**, discovered earlier in the study, was named CSUOH0901 and submitted to the Developmental Therapeutic Program at the National Cancer Institute for screening against 60 human tumor cell lines. It was also investigated for the anti-cancer mechanism and *in vivo* activity in the study.

2.3. CSUOH0901 caused cell population concentrated at sub-G1 and G2 phase

Compound CSUOH0901 significantly inhibited SKBR-3 breast cancer cell growth. It is important to elucidate the anti-cancer mechanisms of the compound. When SKBR-3 cells were treated with 0.5 μM and 5 μM of CSUOH0901, cells were accumulated at G2/M and subG1 phase after 12h. As for 0.25 μM treatment, this phenomenon was observed after 24h (Table 2). The results demonstrate that CSUOH0901 was able to inhibit cell mitosis and induce cell apoptosis at similar dosage to inhibit cell growth. JCC76 has been shown in previous studies to induce cell apoptosis via cytochrome c release [39,40]. It is not surprising that the more potent JCC76 analog CSUOH0901 exhibits better potency to induce cell apoptosis. However, JCC76 did not show good potency to cause cell cycle arrest in previous studies [39,40]. CSUOH0901 obviously exhibited the cell G2/M phase arresting activity. Therefore, the anti-mitosis potency is significantly increased by the structure modification. 0.1 μM CSUOH0901 clearly induced subG1 cell accumulation after 24h treatment, but no G2/M cell accumulation was observed, suggesting that the compound at low concentrations was able to induce cell apoptosis without affecting the cell replication. It is difficult to determine if the cell apoptosis and cell growth arrested by the compound are correlated or not, since the specific molecular targets of CSUOH0901 still remain unclear. Further investigation is needed to identify the anti-cancer molecular targets of these compounds.

2.4. Multi-cancer cell lines growth inhibition and animal acute toxicity studies of CSUOH0901

Due to the structure novelty and potency of CSUOH0901, it was submitted to the Developmental Therapeutic Program at the National Cancer Institute (assigned with code NSC751382), and was selected by NCIDTP for screening against 60 human tumor cell lines, representing leukemia, melanoma, and cancers of the lung, colon, CNS, ovary, renal, prostate, and breast. After 48h treatment, CSUOH0901 dose-dependently inhibited the growth of sixty cell lines from each class of tumor cells. Three dose response parameters are calculated for the experimental agent. Growth inhibition of 50% (GI50) is the drug concentration resulting in a 50% reduction in the net protein increase compared with control cells during the drug incubation. Total growth inhibition (TGI) shows the drug concentration that causes a 100% reduction in the net protein increase during the drug incubation. The LC50 is the concentration of drug resulting in a 50% reduction in protein at the end of the drug treatment as compared to the protein amount present at the time of drug addition.

Values are calculated for each of these three parameters if the requisite level of activity is achieved. The values of these parameters among the 60 different cell lines after 48h treatment are as follows: concentration resulting in 50% growth inhibition (GI₅₀), 0.03 μM to 0.5 μM; concentration resulting in total growth inhibition (TGI), 0.2 μM to 2.0 μM (in approximately one half of the cell lines); concentrations resulting in a 50% reduction in the measured protein level at the end of drug treatment (LC₅₀), above 20 μM in only 3 cell lines (Table 3).

The compound was also tested for the acute toxicity to determine the maximum tolerated dose in nude mice. After a single dose of 400mg/kg, 200mg/kg, or 100mg/kg, the nude mice were observed for a period of 2 weeks. No body weight lost was found in the three mice tested, indicating that the animals were highly tolerable to CSUOH0901.

2.5. *In vivo* investigation

To determine whether the high activity of our compounds at cell culture would translate into *in vivo* active anti-cancer agents, CSUOH0901 as a representative one was investigated in the tumor xenograft nude mice model. SKBR-3 cells do not readily form xenografts in nude mice, therefore we used an colon cancer HT29 xenograft model to investigate the *in vivo* activity of the compound, since it significantly inhibited HT29 cell growth in the *in vitro* study (Developmental Therapeutics Program at National Cancer Institute) with an IC₅₀ of 0.42μM (Table 3). We confirmed the activity of CSUOH0901 in HT29 cells with an MTT cell proliferation assay, and obtained an IC₅₀ of 0.46μM. HT29 xenograft is a well established *in vivo* tumor model, and has been used to test the activity of many anti-cancer drug candidates. Nude mice (three mice per group, two tumors per mouse) bearing HT29 xenografts were given daily (5 times per week) intraperitoneal injections (5mg/kg) of CSUOH0901 for three weeks after the tumor reached a measurable size.

CSUOH0901 treatment significantly decreased the size of the HT29 tumors compared to the control group (Figure 2A). Weights of the mice were not affected by the treatment (Figure 2B), suggesting the low toxicity of the compound. After the treatment, the tumors were removed and weighed. CSUOH0901 significantly decreased the tumor weights as well (Figure 2C). The results reveal that CSUOH0901 is active *in vivo* and could be a promising anti-cancer drug candidate.

2.6. Pharmacokinetic study

CSUOH0901 exhibited potent *in vitro* and *in vivo* anti-tumor activity. To support future further pharmacological and toxicological study, a pharmacokinetic study of the compound was also performed. CSUOH0901 was administrated to rats intraperitoneally at a dose of 20mg/kg. Blood samples (150 μL each) were collected from the saphenous veins and femoral veins into heparized tubes at 0 hr (before drug administration) and at 0.25, 0.5, 1, 2, 4, 8 and 24h after dosing. The peripheral blood drug level was then determined with LC-MS/MS. The mean CSUOH0901 concentration in plasma versus time profile was presented in Figure 3. Peak drug concentrations were observed at 2 hr after administration and reached nearly 1500 ng/mL. The pharmacokinetic parameters were calculated by using non-compartmental model. The estimated pharmacokinetic parameters including the terminal

phase elimination half-life ($T_{1/2}$), the area under the plasma concentration time curve (AUC) from time 0 to time of the last measurable concentration ($AUC_{(0-t)}$), the volume of distribution (V_{zF}), the total body clearance (Cl_F), and the mean residence time (MRT) from time 0 to time of the last measurable concentration ($MRT_{(0-t)}$) are listed in table 4. The half life and volume of distribution of the compound is relatively lower compared with more hydrophobic anti-cancer drugs such as Taxol [47], suggesting the compound has better drug like characters than Taxol. The good bioavailability of the compound recommends further drug development of these small molecular anti-cancer agents.

3. Conclusion

The structural modifications of nimesulide have been effective in abolishing its COX-2 inhibiting property and reducing its hepatotoxicity. Amongst the new derivatives synthesised, compounds **5**, **9**, **10** (CSUOH0901), **16**, **18** and **29** have exhibited good growth inhibitory activity against SK-BR-3 breast cancer cells at low-nanomolar concentrations. CSUOH0901 displayed good potency to inhibit the growth of a broad range of cancer cell lines and demonstrated minor animal toxicity. The *in vivo* tumor suppression activity and pharmacokinetic results of CSUOH0901 suggest that the drug candidate has great clinical application potential.

4. Experimental section

4.1. Chemistry

Chemicals were commercially available and used as received without further purification unless otherwise noted. Moisture sensitive reactions were carried out under a dry argon atmosphere in flame-dried glassware. Solvents were distilled before use under argon. Thin-layer chromatography was performed on precoated silica gel F254 plates (Whatman). Silica gel column chromatography was performed using silica gel 60A (Merck, 230-400 Mesh), and hexane/ethyl acetate was used as the elution solvent. Mass spectra were obtained on the Micromass QTOF Electrospray mass spectrometer at Cleveland State University MS facility Center. Melting point was recorded with a Mel-Temp melting point apparatus. All the NMR spectra were recorded on a Varian 400 MHz in either DMSO- d_6 or $CDCl_3$. Chemical shifts (δ) for 1H NMR spectra are reported in parts per million to residual solvent protons. The IR spectra were obtained on a Bruker ALPHA FT-IR spectrometer with ATR module.

For the HPLC analysis, a 1.00 mg/mL stock solution of each standard was prepared in either methanol or acetonitrile. The HPLC system consists of two LC-20AD pumps, a DGU-20A₃ degasser, a SIL-20AC autosampler, and a CBM-20A module (Shimadzu, Tokyo, Japan). The chromatographic separation was performed on a Luna C18 column (2.0 mm \times 150 mm, 5 μ m) with a guard column (2 mm \times 40 mm, 5 μ m) from Phenomenex (Torrance, CA, USA) at room temperature with a flow rate of 0.2 mL/min. Two mobile phases (10mM ammonium acetate in 90% methanol or acetonitrile) were employed to run 15 min. An injection volume of 5-15 μ L was used. The UV detector was set up at 290 and 256nm.

Compounds **a-e** were prepared as described by Su *et al* [41,46] .

General procedure for the preparation of the substituted benzamide 1-39—

K_2CO_3 (5 mmol, 5eq) and substituted acyl chloride (1.2 mmol, 1.2 eq) were successively added to a solution of the aniline **e** (1.0 mmol, 1.0 eq) in 3ml dry 1, 4 -dioxane and the mixture was stirred at room temperature overnight. 10mL H_2O and 3mL saturated aqueous Na_2CO_3 was added to the mixture and it was stirred at room temperature overnight. The precipitated solid was collected by filtration and purified by silica gel column chromatography.

N-[3-(2,5-Dimethyl-benzyloxy)-4-(methanesulfonyl-methyl-amino)-phenyl]-4-nitro-benzamide (1)—

4-Nitro-benzoyl chloride was used and it was stirred at room temperature overnight. Pale yellow solid, melting point 206-209 °C, yield 88%: 1H -NMR (400 MHz, DMSO- d_6) δ 10.68 (1H, s), 8.41 (2H, d, $J = 8.0$ Hz), 8.21 (2H, d, $J = 8.2$ Hz), 7.75 (1H, s), 7.44 (1H, d, $J = 8.4$ Hz), 7.33(2H, m), 7.15(1H, d, $J = 7.8$ Hz), 7.09(1H, d, $J = 7.8$ Hz), 5.11 (2H, s), 3.12 (3H, s), 2.88 (3H, s), 2.32 (3H, s), 2.28 (3H, s); HRMS calculated for $C_{24}H_{26}N_2NaO_4S$ $[M+Na]^+$ 461.1511, found: 461.1511.

N-[3-(2,5-Dimethyl-benzyloxy)-4-(methanesulfonyl-methyl-amino)-phenyl]-3-nitro-benzamide (2)—

3-Nitro-benzoyl chloride was used and it was stirred at room temperature overnight. White solid, melting point 163-165 °C, yield 86%: 1H -NMR (400 MHz, DMSO- d_6) δ 10.70 (1H, s), 8.80 (1H, s), 8.48 (1H, d, $J = 8.0$ Hz), 8.43 (1H, d, $J = 8.0$ Hz), 7.89 (1H, dd, $J = 7.8, 7.8$ Hz), 7.75 (1H, s), 7.45 (1H, d, $J = 8.6$ Hz), 7.34(2H, m), 7.15(1H, d, $J = 7.4$ Hz), 7.09 (1H, d, $J = 7.5$ Hz), 5.12 (2H, s), 3.12 (3H, s), 2.88 (3H, s), 2.33 (3H, s), 2.28 (3H, s). ESI-MS (m/z) calculated for $C_{24}H_{24}N_3O_6S$ $[M+H]^+$: 482.1, found: 481.9

4-Chloro-N-[3-(2,5-dimethyl-benzyloxy)-4-(methanesulfonyl-methyl-amino)-phenyl]-3-nitro-benzamide (3)—

4-Chloro-3-nitro-benzoyl chloride was used and it was stirred at room temperature overnight. White solid, melting point 204-206 °C, yield 82%: 1H -NMR (400 MHz, DMSO- d_6) δ 10.65 (1H, s), 8.65 (1H, s), 8.28 (1H, d, $J = 8.4$ Hz), 8.01 (1H, d, $J = 8.4$ Hz), 7.72 (1H, s), 7.42 (1H, d, $J = 8.4$ Hz), 7.33(2H, m), 7.15(1H, d, $J = 7.7$ Hz), 7.09 (1H, d, $J = 7.4$ Hz), 5.11 (2H, s), 3.12 (3H, s), 2.87 (3H, s), 2.32 (3H, s), 2.28 (3H, s). ESI-MS calculated for $C_{24}H_{23}ClN_3O_6S$ $[M+H]^+$: 516.1, found: 515.8

3,4-Dichloro-N-[3-(2,5-dimethyl-benzyloxy)-4-(methanesulfonyl-methyl-amino)-phenyl]-benzamide (4)—

3,4-Dichloro-benzoyl chloride was used and it was stirred at room temperature overnight. White solid, melting point 177-179 °C, yield 69%: 1H -NMR (400 MHz, DMSO- d_6) δ 10.51 (1H, s), 8.23 (1H, s), 7.97 (1H, d, $J = 8.4$ Hz), 7.85 (1H, d, $J = 8.4$ Hz), 7.73 (1H, s), 7.42 (1H, d, $J = 7.6$ Hz), 7.31(2H, m), 7.15(1H, d, $J = 7.7$ Hz), 7.09 (1H, d, $J = 7.6$ Hz), 5.10 (2H, s), 3.12 (3H, s), 2.87 (3H, s), 2.32 (3H, s), 2.28 (3H, s). ESI-MS calculated for $C_{24}H_{23}Cl_2N_2O_4S$ $[M+H]^+$: 505.1, found: 504.8

Naphthalene-2-carboxylic acid [3-(2,5-dimethyl-benzyloxy)-4-(methanesulfonyl-methyl-amino)-phenyl]-amide (5)—

Naphthalene-2-carbonyl chloride was used and it was stirred at room temperature for three days. White solid, melting point 133-136 °C, yield 72%: IR $\nu = 3314$ (N-H), 1649 (C=O), 1595, 1509 (aromatic

C=C). $^1\text{H-NMR}$ (400 MHz, $\text{DMSO-}d_6$) δ 10.56 (1H, s), 8.60 (1H, s), 8.12 (4H, m), 7.82 (1H, s), 7.67 (2H, m), 7.50 (1H, d, $J = 8.5$ Hz), 7.33 (2H, m), 7.16 (1H, d, $J = 7.8$ Hz), 7.10 (1H, d, $J = 7.3$ Hz), 5.13 (2H, s), 3.13 (3H, s), 2.88 (3H, s), 2.34 (3H, s), 2.29 (3H, s). $^{13}\text{C-NMR}$ (100 MHz, $\text{DMSO-}d_6$) δ 165.581, 155.169, 148.112, 140.164, 134.702, 134.229, 134.084, 133.100, 131.925, 130.956, 130.003, 129.133, 128.874, 128.660, 127.989, 127.951, 127.836, 127.600, 126.829, 124.663, 124.297, 112.289, 105.348, 68.106, 37.623, 37.509, 20.520, 17.873. ESI-MS calculated for $\text{C}_{28}\text{H}_{27}\text{N}_2\text{O}_4\text{S}$ $[\text{M}+\text{H}]^+$: 487.2, found: 486.9

Biphenyl-4-carboxylic acid [3-(2,5-dimethyl-benzyloxy)-4-(methanesulfonyl-methyl-amino)-phenyl]-amide (6)—Biphenyl-4-carbonyl chloride was used and it was stirred at room temperature for three days. White solid, melting point 136-139 °C, yield 73%: $^1\text{H-NMR}$ (400 MHz, $\text{DMSO-}d_6$) δ 10.42 (1H, s), 8.09 (2H, d, $J = 7.9$ Hz), 7.88 (2H, d, $J = 7.8$ Hz), 7.81 (1H, s), 7.79 (2H, d, $J = 7.2$ Hz), 7.54 (4H, m), 7.33 (2H, m), 7.16 (1H, d, $J = 7.7$ Hz), 7.10 (1H, d, $J = 7.5$ Hz), 5.12 (2H, s), 3.12 (3H, s), 2.87 (3H, s), 2.33 (3H, s), 2.28 (3H, s). ESI-MS calculated for $\text{C}_{30}\text{H}_{29}\text{N}_2\text{O}_4\text{S}$ $[\text{M}+\text{H}]^+$: 513.2, found: 512.9

4-Cyano-N-[3-(2,5-dimethyl-benzyloxy)-4-(methanesulfonyl-methyl-amino)-phenyl]-benzamide (7)—4-Cyano-benzoyl chloride was used and it was stirred at room temperature overnight. White solid, melting point 183-187 °C, yield 75%: $^1\text{H-NMR}$ (400 MHz, $\text{DMSO-}d_6$) δ 10.60 (1H, s), 8.13 (2H, d, $J = 8.4$ Hz), 8.06 (2H, d, $J = 8.2$ Hz), 7.75 (1H, d, $J = 1.7$ Hz), 7.43 (1H, dd, $J = 1.9, 8.5$ Hz), 7.32 (2H, m), 7.15 (1H, d, $J = 7.7$ Hz), 7.09 (1H, d, $J = 7.7$ Hz), 5.11 (2H, s), 3.12 (3H, s), 2.87 (3H, s), 2.32 (3H, s), 2.28 (3H, s). ESI-MS calculated for $\text{C}_{25}\text{H}_{24}\text{N}_3\text{O}_4\text{S}$ $[\text{M}+\text{H}]^+$: 462.1, found: 461.9

3-Cyano-N-[3-(2,5-dimethyl-benzyloxy)-4-(methanesulfonyl-methyl-amino)-phenyl]-benzamide (8)—3-Cyano-benzoyl chloride was used and it was stirred at room temperature overnight. White solid, melting point 166-170 °C, yield 71%: $^1\text{H-NMR}$ (400 MHz, $\text{DMSO-}d_6$) δ 10.54 (1H, s), 8.42 (1H, s), 8.27 (1H, d, $J = 7.8$ Hz), 8.10 (1H, d, $J = 7.7$ Hz), 7.80 (2H, m), 7.43 (1H, d, $J = 8.5$ Hz), 7.32 (2H, m), 7.15 (1H, d, $J = 7.7$ Hz), 7.09 (1H, d, $J = 7.8$ Hz), 5.11 (2H, s), 3.12 (3H, s), 2.87 (3H, s), 2.32 (3H, s), 2.28 (3H, s). ESI-MS calculated for $\text{C}_{25}\text{H}_{24}\text{N}_3\text{O}_4\text{S}$ $[\text{M}+\text{H}]^+$: 462.1, found: 461.9

4-Bromo-N-[3-(2,5-dimethyl-benzyloxy)-4-(methanesulfonyl-methyl-amino)-phenyl]-benzamide (9)—4-Bromo-benzoyl chloride was used and it was stirred at room temperature overnight. White solid, melting point 196-197 °C, yield 80%: IR $\nu = 3338$ (N-H), 1654 (C=O), 1593, 1507 (aromatic C=C). $^1\text{H-NMR}$ (400 MHz, $\text{DMSO-}d_6$) δ 10.43 (1H, s), 7.93 (2H, d, $J = 8.2$ Hz), 7.79 (2H, d, $J = 8.5$ Hz), 7.75 (1H, s), 7.40 (1H, m), 7.31 (2H, m), 7.15 (1H, d, $J = 7.7$ Hz), 7.09 (1H, d, $J = 7.7$ Hz), 5.10 (2H, s), 3.11 (3H, s), 2.87 (3H, s), 2.32 (3H, s), 2.28 (3H, s). $^{13}\text{C-NMR}$ (100 MHz, $\text{DMSO-}d_6$) δ 164.551, 155.146, 139.874, 134.702, 134.046, 133.657, 133.100, 131.368, 130.948, 130.003, 129.720, 129.141, 128.668, 125.456, 124.815, 112.335, 105.393, 68.114, 37.623, 37.486, 20.520, 17.866. ESI-MS calculated for $\text{C}_{24}\text{H}_{24}\text{BrN}_2\text{O}_4\text{S}$ $[\text{M}+\text{H}]^+$: 515.1, found: 514.8

Benzo[1,3]dioxole-5-carboxylic acid [3-(2,5-dimethyl-benzyloxy)-4-(methanesulfonyl-methyl-amino)-phenyl]-amide (10)—1,3-Dihydro-

isobenzofuran-5-carbonyl chloride was used and it was stirred at room temperature overnight. White solid, melting point 159-165 °C(decomposed), yield 71%: IR ν = 3354 (N-H), 1653 (C=O), 1596, 1506 (aromatic C=C). ¹H-NMR (400 MHz, DMSO-*d*₆) δ 10.18 (1H, s), 7.75 (1H, s), 7.60 (1H, d, *J* = 8.1 Hz), 7.52 (1H, s), 7.41 (1H, dd, *J* = 1.5, 8.4 Hz), 7.31 (1H, s), 7.28 (1H, d, *J* = 8.5 Hz), 7.15(1H, d, *J* = 7.6 Hz), 7.09 (2H, d, *J* = 8.0 Hz), 6.15 (2H, s), 5.09 (2H, s), 3.11 (3H, s), 2.86 (3H, s), 2.32 (3H, s), 2.28 (3H, s). ¹³C-NMR (100 MHz, DMSO-*d*₆) δ 164.475, 155.100, 150.088, 147.311, 140.186, 134.686, 134.068, 133.107, 130.857, 129.995, 129.171, 128.660, 128.362, 124.472, 122.832, 112.206, 107.873, 107.598, 105.271, 101.770, 68.076, 37.585, 37.493, 20.513, 17.858. ESI-MS calculated for C₂₅H₂₅N₂O₆S [M+H]⁺ : 481.1, found: 480.8

N-[3-(2,5-Dimethyl-benzyloxy)-4-(methanesulfonyl-methyl-amino)-phenyl]-3,4,5-trimethoxy-benzamide (11)—3,4,5-Trimethoxy-benzoyl chloride was used and it was stirred at room temperature overnight. White solid, melting point 187-189 °C, yield 93%: ¹H-NMR (400 MHz, DMSO-*d*₆) δ 10.26 (1H, s), 7.76 (1H, s), 7.36 (5H, m), 7.13(1H, d, *J* = 7.7 Hz), 7.09 (1H, d, *J* = 7.7 Hz), 5.11 (2H, s), 3.89 (6H, s), 3.75 (3H, s), 3.12 (3H, s), 2.87 (3H, s), 2.32 (3H, s), 2.28 (3H, s). ESI-MS calculated for C₂₇H₃₁N₂O₇S [M+H]⁺ : 527.2, found: 526.9

N-[3-(2,5-Dimethyl-benzyloxy)-4-(methanesulfonyl-methyl-amino)-phenyl]-propionamide (12)—Propionoyl chloride was used and it was stirred at room temperature overnight. White solid, melting point 168-170 °C, yield 88%: ¹H-NMR (400 MHz, DMSO-*d*₆) δ 10.00 (1H, s), 7.58 (1H, s), 7.28 (1H, s), 7.23 (1H, d, *J* = 8.5 Hz), 7.16(1H, s), 7.14(1H, d, *J* = 7.6 Hz), 7.08 (1H, d, *J* = 7.6 Hz), 5.06 (2H, s), 3.08 (3H, s), 2.84 (3H, s), 2.36 (2H, dd, *J* = 7.5, 6.4 Hz), 2.30 (3H, s), 2.27 (3H, s), 1.10 (3H, dd, *J* = 7.5, 7.6 Hz). ESI-MS calculated for C₂₀H₂₅N₂O₄S [M+H]⁺ : 389.2, found: 388.9

Hexadecanoic acid [3-(2,5-dimethyl-benzyloxy)-4-(methanesulfonyl-methyl-amino)-phenyl]-amide (13)—Hexadecanoyl chloride was used and it was stirred at room temperature overnight. White solid, melting point 134-140 °C(decomposed), yield 98%: ¹H-NMR (400 MHz, DMSO-*d*₆) δ 10.03 (1H, s), 7.59 (1H, s), 7.28 (1H, s), 7.20 (4H, m), 5.06 (2H, s), 3.08 (3H, s), 2.84 (3H, s), 2.30 (3H, s), 2.27 (3H, s), 1.58 (2H, br), 1.23 (26H, br), 0.87 (3H, dd, *J* = 5.1, 6.6 Hz).

2,4-Dichloro-N-[3-(2,5-dimethyl-benzyloxy)-4-(methanesulfonyl-methyl-amino)-phenyl]-benzamide (14)—2,4-Dichloro-benzoyl chloride was used and it was stirred at room temperature overnight. White solid, melting point 163-166 °C, yield 80%: ¹H-NMR (400 MHz, DMSO-*d*₆) δ 10.68 (1H, s), 7.79 (1H, s), 7.61 (1H, s), 7.64 (1H, d, *J* = 8.2 Hz), 7.59 (1H, d, *J* = 8.4 Hz), 7.29 (3H, br), 7.14(1H, d, *J* = 7.4 Hz), 7.08 (1H, d, *J* = 7.4 Hz), 5.09 (2H, s), 3.12 (3H, s), 2.87 (3H, s), 2.31 (3H, s), 2.27 (3H, s). ESI-MS calculated for C₂₄H₂₃Cl₂N₂O₄S [M+H]⁺ : 505.1, found: 504.8

N-[3-(2,5-Dimethyl-benzyloxy)-4-(methanesulfonyl-methyl-amino)-phenyl]-3-trifluoromethyl-benzamide (15)—3-Trifluoromethyl-benzoyl chloride was used and it was stirred at room temperature overnight. White solid, melting point 179-181 °C, yield

93%: $^1\text{H-NMR}$ (400 MHz, $\text{DMSO-}d_6$) δ 10.61 (1H, s), 8.30 (2H, m), 8.00 (1H, d, $J = 7.6$ Hz), 7.81 (2H, m), 7.44 (1H, d, $J = 8.5$ Hz), 7.32 (1H, s), 7.32 (1H, d, $J = 8.4$ Hz), 7.15 (1H, d, $J = 7.6$ Hz), 7.09 (1H, d, $J = 7.6$ Hz), 5.11 (2H, s), 3.12 (3H, s), 2.87 (3H, s), 2.32 (3H, s), 2.28 (3H, s). ESI-MS calculated for $\text{C}_{25}\text{H}_{24}\text{F}_3\text{N}_2\text{O}_4\text{S}$ $[\text{M}+\text{H}]^+$: 505.1, found: 504.9

N-[3-(2,5-Dimethyl-benzyloxy)-4-(methanesulfonyl-methyl-amino)-phenyl]-3,4-dimethoxy-benzamide (16)—3,4-Dimethoxy-benzoyl chloride was used and it was stirred at room temperature overnight. White solid, melting point 184-186 °C, yield 93 %: IR $\nu = 3352$ (N-H), 1649 (C=O), 1599, 1505 (aromatic C=C). $^1\text{H-NMR}$ (400 MHz, CDCl_3) δ 8.025 (2H, m), 7.510 (1H, $J = 2$ Hz), 7.434 (1H, dd, $J = 8.4, 2$ Hz), 7.309 (1H, $J = 8.8$ Hz), 7.162 (1H, s), 7.109 (2H, m), 6.919 (1H, d, $J = 8.4$ Hz), 6.832 (1H, dd, $J = 2, 8.4$ Hz), 5.067 (2H, s), 3.957 (3H, s), 3.952 (3H, s), 3.195 (3H, s), 2.707 (3H, s), 2.335 (3H, s), 2.320 (3H, s). $^{13}\text{C-NMR}$ (100 MHz, $\text{DMSO-}d_6$) δ 164.933, 155.138, 151.682, 148.242, 140.278, 134.709, 134.099, 133.130, 130.865, 130.010, 129.194, 128.683, 126.616, 124.457, 120.948, 112.312, 110.955, 110.749, 105.355, 68.114, 55.588, 55.527, 37.608, 37.516, 20.520, 17.873. ESI-MS calculated for $\text{C}_{26}\text{H}_{29}\text{N}_2\text{O}_6\text{S}$ $[\text{M}+\text{H}]^+$: 497.2, found: 496.9

N-[3-(2,5-Dimethyl-benzyloxy)-4-(methanesulfonyl-methyl-amino)-phenyl]-(3,4-dimethoxyphenyl)-acetamide (17)—(3,4-Dimethoxy-phenyl)-acetyl chloride was used and it was stirred at room temperature overnight. White solid, melting point 149-152 °C, yield 95%: $^1\text{H-NMR}$ (400 MHz, CDCl_3) δ 7.844 (1H, d, $J = 2.4$ Hz), 7.240 (2H, m), 7.141 (1H, s), 7.103 (2H, m), 6.893 (2H, m), 6.825 (1H, d, $J = 1.6$ Hz), 6.555 (1H, dd, $J = 2.4, 8.4$ Hz), 5.029 (2H, s), 3.907 (3H, s), 3.898 (3H, s), 3.696 (2H, s), 3.157 (3H, s), 2.683 (3H, s), 2.322 (3H, s), 2.312 (3H, s). ESI-MS calculated for $\text{C}_{27}\text{H}_{31}\text{N}_2\text{O}_6\text{S}$ $[\text{M}+\text{H}]^+$: 511.2, found: 510.9

N-[3-(2,5-Dimethyl-benzyloxy)-4-(methanesulfonyl-methyl-amino)-phenyl]-4-methoxy-benzamide (18)—4-Methoxy-benzoyl chloride was used and it was stirred at room temperature overnight. White solid, melting point 175-178 °C, yield 96%: IR $\nu = 3345$ (N-H), 1649 (C=O), 1602, 1506 (aromatic C=C). $^1\text{H-NMR}$ (400 MHz, CDCl_3) δ 8.022 (1H, d, $J = 2.4$ Hz), 7.864 (3H, m), 7.330 (1H, d, $J = 8.4$ Hz), 7.175 (1H, s), 7.113 (2H, m), 6.995 (2H, m), 6.823 (1H, dd, $J = 2.4, 8.4$ Hz), 5.086 (2H, s), 3.886 (3H, s), 3.198 (3H, s), 2.712 (3H, s), 2.345 (3H, s), 2.325 (3H, s). $^{13}\text{C-NMR}$ (100 MHz, $\text{DMSO-}d_6$) δ 164.887, 161.920, 155.107, 140.324, 134.694, 134.091, 133.107, 130.857, 129.995, 129.552, 129.171, 128.660, 126.600, 124.380, 113.541, 112.190, 105.264, 68.083, 55.351, 37.593, 37.509, 20.513, 17.866. ESI-MS calculated for $\text{C}_{25}\text{H}_{27}\text{N}_2\text{O}_5\text{S}$ $[\text{M}+\text{H}]^+$: 467.2, found: 466.9

N-[3-(2,5-Dimethyl-benzyloxy)-4-(methanesulfonyl-methyl-amino)-phenyl]-2-methoxy-benzamide (19)—2-Methoxy-benzoyl chloride was used and it was stirred at room temperature overnight. White solid, melting point 147-149 °C, yield 97%: $^1\text{H-NMR}$ (400 MHz, CDCl_3) δ 9.932 (1H, s), 8.283 (1H, dd, $J = 2, 8$ Hz), 8.202 (1H, d, $J = 2.4$ Hz), 7.535 (1H, m), 7.342 (1H, d, $J = 8.4$ Hz), 7.106 (5H, m), 6.759 (1H, dd, $J = 2, 8.4$ Hz), 5.119 (2H, s), 4.079 (3H, s), 3.201 (3H, s), 2.706 (3H, s), 2.361 (3H, s), 2.329 (3H, s). ESI-MS calculated for $\text{C}_{25}\text{H}_{27}\text{N}_2\text{O}_5\text{S}$ $[\text{M}+\text{H}]^+$: 467.2, found: 466.9

N-[3-(2,5-Dimethyl-benzyloxy)-4-(methanesulfonyl-methyl-amino)-phenyl]-3-methoxy-benzamide (20)—3-Methoxy-benzoyl chloride was used and it was stirred at room temperature overnight. White solid, melting point 143-144 °C, yield 91%: ¹H-NMR (400 MHz, CDCl₃) δ 8.021 (1H, d, *J* = 2.4 Hz), 7.938 (1H, s), 7.445 (1H, m), 7.406 (2H, m), 7.344 (1H, d, *J* = 8.4 Hz), 7.177 (1H, s), 7.121 (3H, m), 6.848 (1H, dd, *J* = 2.4, 8.4 Hz), 5.093 (2H, s), 3.885 (3H, s), 3.201 (3H, s), 2.714 (3H, s), 2.349 (3H, s), 2.327 (3H, s). ESI-MS calculated for C₂₅H₂₇N₂O₅S [M+H]⁺: 467.2, found: 466.9

N-[3-(2,5-Dimethyl-benzyloxy)-4-(methanesulfonyl-methyl-amino)-phenyl]-3-methoxy-2,4,5-trifluorobenzamide (21)—3-Methoxy-2,4,5-trifluorobenzoyl chloride was used and it was stirred at room temperature overnight. White solid, melting point 166-169 °C, yield 98%: ¹H-NMR (400 MHz, CDCl₃) δ 8.381 (1H, d, *J* = 14.8 Hz), 7.927 (1H, s), 7.680 (1H, m), 7.362 (1H, d, *J* = 8.4 Hz), 7.180 (1H, s), 7.115 (2H, m), 6.880 (1H, d, *J* = 8.4 Hz), 5.094 (2H, s), 4.106 (3H, s), 3.199 (3H, s), 2.719 (3H, s), 2.358 (3H, s), 2.328 (3H, s). ESI-MS calculated for C₂₅H₂₄F₃N₂O₅S [M+H]⁺: 521.1, found: 520.9

N-[3-(2,5-Dimethyl-benzyloxy)-4-(methanesulfonyl-methyl-amino)-phenyl]-2-ethyl-butyramide (22)—2-Ethyl-butyryl chloride was used and it was stirred at room temperature overnight. White solid, melting point 151-154 °C, yield 96%: ¹H-NMR (400 MHz, CDCl₃) δ 8.049 (1H, d, *J* = 2.4 Hz), 7.296 (1H, s), 7.275 (1H, s), 7.157 (1H, s), 7.108 (2H, m), 6.673 (1H, dd, *J* = 2.4, 8.8 Hz), 5.064 (2H, s), 3.172 (3H, s), 2.691 (3H, s), 2.339 (3H, s), 2.318 (3H, s), 2.08 (1H, m), 1.70 (4H, m), 0.970 (6H, t, *J* = 7.6 Hz). ESI-MS calculated for C₂₃H₃₁N₂O₄S [M+H]⁺: 431.2, found: 430.9

N-[3-(2,5-Dimethyl-benzyloxy)-4-(methanesulfonyl-methyl-amino)-phenyl]-cyclopentanecarboxamide (23)—Cyclopentane carbonyl chloride was used and it was stirred at room temperature overnight. White solid, melting point 170-172 °C, yield 93%: ¹H-NMR (400 MHz, CDCl₃) δ 7.998 (1H, d, *J* = 2 Hz), 7.357 (1H, s), 7.265 (1H, d, *J* = 8.4 Hz), 7.149 (1H, s), 7.106 (2H, m), 6.641 (1H, dd, *J* = 2.4, 8.4 Hz), 5.045 (2H, s), 3.169 (3H, s), 2.703 (1H, m), 2.690 (3H, s), 2.327 (3H, s), 2.318 (3H, s), 1.921 (4H, m), 1.80 (2H, m), 1.641 (2H, m). ESI-MS calculated for C₂₃H₂₉N₂O₄S [M+H]⁺: 429.2, found: 428.9

N-[3-(2,5-Dimethyl-benzyloxy)-4-(methanesulfonyl-methyl-amino)-phenyl]-2-phenyl-acetamide (24)—Phenylacetyl chloride was used and it was stirred at room temperature overnight. White solid, melting point 185-186 °C, yield 99%: ¹H-NMR (400 MHz, CDCl₃) δ 7.867 (1H, d, *J* = 2.4 Hz), 7.399 (5H, m), 7.239 (1H, d, *J* = 8.4 Hz), 7.187 (1H, s), 7.102 (3H, m), 6.535 (1H, dd, *J* = 3, 9 Hz), 5.026 (2H, s), 3.757 (2H, s), 3.156 (3H, s), 2.679 (3H, s), 2.320 (3H, s), 2.312 (3H, s). ESI-MS calculated for C₂₅H₂₇N₂O₄S [M+H]⁺: 451.2, found: 450.9

N-[3-(2,5-Dimethyl-benzyloxy)-4-(methanesulfonyl-methyl-amino)-phenyl]-1-naphthalenecarboxamide (25)—1-Naphthoyl chloride was used and it was stirred at room temperature overnight. White solid, melting point 164-168 °C, yield 83%: ¹H-NMR (400 MHz, CDCl₃) δ 8.350 (1H, d, *J* = 8 Hz), 8.105 (1H, s), 7.992 (1H, d, *J* = 8.4 Hz), 7.921 (1H, m), 7.865 (1H, s), 7.741 (1H, d, *J* = 6.4 Hz), 7.543 (3H, m), 7.345 (1H, d, *J* = 8.4

Hz), 7.199 (1H, s), 7.116 (2H, m), 6.845 (1H, dd, $J = 2, 8.4$ Hz), 5.129 (2H, s), 3.208 (3H, s), 2.711 (3H, s), 2.365 (3H, s), 2.336 (3H, s). ESI-MS calculated for $C_{28}H_{29}N_2O_4S$ $[M+H]^+$: 489.2, found: 489.1

N-[3-(2,5-Dimethyl-benzyloxy)-4-(methanesulfonyl-methyl-amino)-phenyl]-3,5-bis(trifluoromethyl)benzamide (26)—3,5-Bis(trifluoromethyl)benzoyl chloride was used and it was stirred at room temperature overnight. White solid, melting point 191-192 °C, yield 93%: 1H -NMR (400 MHz, $CDCl_3$) δ 8.348 (3H, s), 8.067 (1H, s), 7.892 (1H, s), 7.289 (1H, d, $J = 10.8$ Hz), 7.173 (1H, s), 7.108 (2H, m), 6.908 (1H, d, $J = 8.4$ Hz), 5.051 (2H, s), 3.193 (3H, s), 2.754 (3H, s), 2.342 (3H, s), 2.309 (3H, s). ESI-MS calculated for $C_{26}H_{23}F_6N_2O_4S$ $[M+H]^+$: 573.1, found: 572.9

N-[3-(2,5-Dimethyl-benzyloxy)-4-(methanesulfonyl-methyl-amino)-phenyl]-3-bromobenzamide (27)—3-Bromobenzoyl chloride was used and it was stirred at room temperature overnight. White solid, melting point 176-178 °C, yield 99%: 1H -NMR (400 MHz, $CDCl_3$) δ 8.022 (2H, m), 7.947 (1H, d, $J = 2.4$ Hz), 7.810 (1H, d, $J = 8$ Hz), 7.698 (1H, d, $J = 8$ Hz), 7.404 (1H, t, $J = 8$ Hz), 7.320 (1H, d, $J = 8.4$ Hz), 7.172 (1H, s), 7.114 (2H, m), 6.867 (1H, dd, $J = 2.4, 8.4$ Hz), 5.072 (2H, s), 3.199 (3H, s), 2.726 (3H, s), 2.343 (3H, s), 2.322 (3H, s). ESI-MS calculated for $C_{24}H_{24}BrN_2O_4S$ $[M+H]^+$: 515.1, found: 514.8

N-[3-(2,5-Dimethyl-benzyloxy)-4-(methanesulfonyl-methyl-amino)-phenyl]-4-chlorobenzamide (28)—4-Chloro-benzoyl chloride was used and it was stirred at room temperature overnight. White solid, melting point 171-174 °C, yield 99%: 1H -NMR (400 MHz, $CDCl_3$) δ 7.967 (1H, d, $J = 2.4$ Hz), 7.951 (1H, s), 7.838 (2H, m), 7.491 (2H, m), 7.335 (1H, d, $J = 8.4$ Hz), 7.176 (1H, s), 7.111 (2H, m), 6.850 (1H, dd, $J = 2.4, 8.4$ Hz), 5.084 (2H, s), 3.204 (3H, s), 2.725 (3H, s), 2.348 (3H, s), 2.326 (3H, s). ESI-MS calculated for $C_{24}H_{24}ClN_2O_4S$ $[M+H]^+$: 471.1, found: 470.8

N-[3-(2,5-Dimethyl-benzyloxy)-4-(methanesulfonyl-methyl-amino)-phenyl]-4-iodobenzamide (29)—4-Iodo-benzoyl chloride was used and it was stirred at room temperature overnight. White solid, melting point 207-209 °C, yield 96%: IR $\nu = 3308$ (N-H), 1653 (C=O), 1594, 1518 (aromatic C=C). 1H -NMR (400 MHz, $DMSO-d_6$) δ 10.408 (1H, s), 7.939 (2H, m), 7.748 (3H, m), 7.398 (1H, dd, $J = 2.4, 8.8$ Hz), 7.291 (2H, m), 7.124 (2H, m), 5.090 (2H, s), 3.105 (3H, s), 2.858 (3H, s), 2.311 (3H, s), 2.270 (3H, s). ^{13}C -NMR (100 MHz, $DMSO-d_6$) δ 164.811, 155.130, 139.912, 137.204, 134.686, 134.046, 133.954, 133.092, 130.926, 129.995, 129.514, 129.133, 128.660, 124.762, 112.328, 105.386, 99.474, 68.106, 37.615, 37.486, 20.513, 17.858. ESI-MS calculated for $C_{24}H_{24}IN_2O_4S$ $[M+H]^+$: 563.1, found: 562.8

N-[3-(2,5-Dimethyl-benzyloxy)-4-(methanesulfonyl-methyl-amino)-phenyl]-4-methylsulfanyl-benzamide (30)—4-Methylsulfanyl-benzoyl chloride was used and it was stirred at room temperature overnight. White solid, melting point 195-197 °C, yield 92%: 1H -NMR (400 MHz, $CDCl_3$) δ 8.017 (1H, d, $J = 2.4$ Hz), 7.868 (1H, s), 7.799 (2H, m), 7.327 (3H, m), 7.177 (1H, s), 7.116 (2H, m), 6.834 (1H, dd, $J = 2, 8.4$ Hz), 5.093 (2H,

s), 3.200 (3H, s), 2.715 (3H, s), 2.543 (3H, s), 2.348 (3H, s), 2.326 (3H, s). ESI-MS calculated for $C_{25}H_{27}N_2O_4S_2$ $[M+H]^+$: 483.1, found: 483.0

N-[3-(2,5-Dimethyl-benzyloxy)-4-(methanesulfonyl-methyl-amino)-phenyl]-4-dimethylamino-benzamide (31)—4-Dimethylamino-benzoyl chloride was used and it was stirred at room temperature overnight. White solid, melting point 171-172 °C, yield 66%: 1H -NMR (400 MHz, $CDCl_3$) δ 8.086 (1H, d, $J = 2.4$ Hz), 7.823 (1H, s), 7.789 (2H, d, $J = 9.2$ Hz), 7.321 (1H, d, $J = 8.4$ Hz), 7.174 (1H, s), 7.110 (2H, m), 6.790 (1H, dd, $J = 2, 8.4$ Hz), 6.720 (2H, d, $J = 9.2$ Hz), 5.089 (2H, s), 3.194 (3H, s), 3.064 (6H, s), 2.703 (3H, s), 2.343 (3H, s), 2.324 (3H, s). ESI-MS calculated for $C_{26}H_{30}N_3O_4S$ $[M+H]^+$: 480.2, found: 479.9

N-[3-(2,5-Dimethyl-benzyloxy)-4-(methanesulfonyl-methyl-amino)-phenyl]-4-ethoxy-benzamide (32)—4-Ethoxy-benzoyl chloride was used and it was stirred at room temperature overnight. White solid, melting point 184-185 °C, yield 70%: 1H -NMR (400 MHz, $CDCl_3$) δ 8.014 (1H, d, $J = 2$ Hz), 7.925 (1H, s), 7.847 (2H, m), 7.316 (1H, d, $J = 8.4$ Hz), 7.168 (1H, s), 7.110 (2H, m), 6.972 (2H, m), 6.822 (1H, dd, $J = 2.4, 8.4$ Hz), 5.074 (2H, s), 4.111 (2H, q, $J = 7.2$ Hz), 3.195 (3H, s), 2.708 (3H, s), 2.340 (3H, s), 2.320 (3H, s), 1.455 (3H, t, $J = 7.2$ Hz). ESI-MS calculated for $C_{26}H_{29}N_2O_5S$ $[M+H]^+$: 481.2, found: 480.9

N-[3-(2,5-Dimethyl-benzyloxy)-4-(methanesulfonyl-methyl-amino)-phenyl]-4-ethyl-benzamide (33)—4-Ethyl-benzoyl chloride was used and it was stirred at room temperature overnight. Pale yellow solid, melting point 178-181 °C, yield 64%: 1H -NMR (400 MHz, $CDCl_3$) δ 8.038 (1H, d, $J = 2.4$ Hz), 7.987 (1H, s), 7.814 (2H, m), 7.327 (3H, m), 7.173 (1H, s), 7.112 (2H, m), 6.834 (1H, dd, $J = 2.4, 8.4$ Hz), 5.083 (2H, s), 3.197 (3H, s), 2.733 (2H, q, $J = 7.6$ Hz), 2.708 (3H, s), 2.343 (3H, s), 2.324 (3H, s), 1.276 (3H, t, $J = 7.6$ Hz). ESI-MS calculated for $C_{26}H_{29}N_2O_4S$ $[M+H]^+$: 465.2, found: 464.9

N-[3-(2,5-Dimethyl-benzyloxy)-4-(methanesulfonyl-methyl-amino)-phenyl]-4-trifluoromethyl-benzamide (34)—4-Trifluoromethyl-benzoyl chloride was used and it was stirred at room temperature overnight. White solid, melting point 215-218 °C, yield 84%: 1H -NMR (400 MHz, $DMSO-d_6$) δ 10.590 (1H, s), 8.157 (2H, d, $J = 8$ Hz), 7.941 (2H, d, $J = 8$ Hz), 7.753 (1H, d, $J = 2.4$ Hz), 7.419 (1H, dd, $J = 2.4, 8.8$ Hz), 7.307 (2H, m), 7.129 (2H, m), 5.107 (2H, s), 3.116 (3H, s), 2.871 (3H, s), 2.319 (3H, s), 2.275 (3H, s). ESI-MS calculated for $C_{25}H_{24}F_3N_2O_4S$ $[M+H]^+$: 505.1, found: 504.9

N-[3-(2,5-Dimethyl-benzyloxy)-4-(methanesulfonyl-methyl-amino)-phenyl]-4-trifluoromethoxy-benzamide (35)—4-Trifluoromethoxy-benzoyl chloride was used and it was stirred at room temperature overnight. White solid, melting point 194-197 °C, yield 79%: 1H -NMR (400 MHz, $CDCl_3$) δ 7.954 (4H, m), 7.350 (3H, m), 7.177 (1H, s), 7.117 (2H, m), 7.848 (1H, dd, $J = 2.4, 8.4$ Hz), 5.088 (2H, s), 3.204 (3H, s), 2.724 (3H, s), 2.349 (3H, s), 2.324 (3H, s). ESI-MS calculated for $C_{25}H_{24}F_3N_2O_5S$ $[M+H]^+$: 521.1, found: 520.9

N-[3-(2,5-Dimethyl-benzyloxy)-4-(methanesulfonyl-methyl-amino)-phenyl]-4-methyl-benzamide (36)—4-Methyl-benzoyl chloride was used and it was stirred at room

temperature overnight. White solid, melting point 170-173 °C, yield 69%: ¹H-NMR (400 MHz, CDCl₃) δ 8.032 (1H, d, *J* = 2 Hz), 7.956 (1H, s), 7.786 (2H, m), 7.339 (1H, s), 7.309 (2H, d, *J* = 7.6 Hz), 7.175 (1H, s), 7.113 (2H, m), 6.834 (1H, dd, *J* = 2, 8.4 Hz), 5.084 (2H, s), 3.198 (3H, s), 2.710 (3H, s), 2.438 (3H, s), 2.344 (3H, s), 2.324 (3H, s). ESI-MS calculated for C₂₅H₂₇N₂O₄S [M+H]⁺ : 451.2, found: 450.9

N-[3-(2,5-Dimethyl-benzyloxy)-4-(methanesulfonyl-methyl-amino)-phenyl]-furan-2-carboxamide (37)—

2-Furoyl chloride was used and it was stirred at room temperature overnight. White solid, melting point 156-157 °C, yield 66%: ¹H-NMR (400 MHz, CDCl₃) δ 8.159 (1H, s), 8.004 (1H, d, *J* = 2.4 Hz), 7.551 (1H, m), 7.352 (1H, d, *J* = 8.4 Hz), 7.268 (1H, m), 7.180 (1H, s), 7.119 (2H, m), 6.875 (1H, dd, *J* = 2.4, 8.8 Hz), 6.595 (1H, dd, *J* = 2, 3.6 Hz), 5.091 (2H, s), 3.202 (3H, s), 2.720 (3H, s), 2.351 (3H, s), 2.328 (3H, s). ESI-MS calculated for C₂₂H₂₃N₂O₅S [M+H]⁺ : 427.1, found: 426.8

N-[3-(2,5-Dimethyl-benzyloxy)-4-(methanesulfonyl-methyl-amino)-phenyl]-thiophene-2-carboxamide (38)—

2-Thiophene carbonyl chloride was used and it was stirred at room temperature overnight. White solid, melting point 163-164 °C, yield 72%: ¹H-NMR (400 MHz, CDCl₃) δ 7.986 (1H, d, *J* = 2.4 Hz), 7.877 (1H, s), 7.668 (1H, dd, *J* = 1.2, 3.6 Hz), 7.589 (1H, dd, *J* = 1.2, 5.2 Hz), 7.323 (1H, d, *J* = 8.4 Hz), 7.144 (4H, m), 6.816 (1H, dd, *J* = 2.4, 8.8 Hz), 5.072 (2H, s), 3.197 (3H, s), 2.718 (3H, s), 2.341 (3H, s), 2.324 (3H, s). ESI-MS calculated for C₂₂H₂₃N₂O₄S₂ [M+H]⁺ : 443.1, found: 442.8

N-[3-(2,5-Dimethyl-benzyloxy)-4-(methanesulfonyl-methyl-amino)-phenyl]-isoxazole-5-carboxamide (39)—

Isoxazole-5-carbonyl chloride was used and it was stirred at room temperature overnight. White solid, melting point 130-138 °C (decomposed), yield 99%: ¹H-NMR (400 MHz, CDCl₃) δ 8.418 (1H, d, *J* = 2 Hz), 8.360 (1H, s), 7.849 (1H, dd, *J* = 2.4 Hz), 7.391 (1H, d, *J* = 8.4 Hz), 7.181 (1H, s), 7.126 (2H, m), 7.060 (1H, d, *J* = 2 Hz), 7.005 (1H, dd, *J* = 2.4, 8.4 Hz), 5.095 (2H, s), 3.211 (3H, s), 2.741 (3H, s), 2.357 (3H, s), 2.329 (3H, s). ESI-MS calculated for C₂₁H₂₂N₃O₅S [M+H]⁺ : 428.1, found: 427.8

4.2. Pharmacological studies

4.2.1. Cell culture

—SKBR-3, HT29 cells were obtained from ATCC (Rockville, MD).

All cells were maintained in RPMI1640 medium supplemented with 10% fetal bovine serum (FBS), 2 mmol/L L-Glutamine, 1 mmol/L sodium pyruvate, 100 U/mL penicillin-streptomycin. FBS was heat inactivated for 30 min in a 56 °C water bath before use. Cell cultures were grown at 37 °C, in a humidified atmosphere of 5% CO₂ in a Heraeus CO₂ incubator.

4.2.2. Cell viability analysis—The effect of nimesulides derivatives on SKBR-3 and HT29 cell viability was assessed by using the 3-(4,5-dimethylthiazol-2-yl)-2,5-diphenyl-2H-tetrazolium bromide assay in six replicates. Cells were grown in RPMI1640 medium in 96-well, flat-bottomed plates for 24 h, and were exposed to various concentrations of JCC76 derivatives dissolved in DMSO (final concentration 0.1%) in media for 48h. Controls received DMSO vehicle at a concentration equal to that in drug-treated cells. The medium was removed, replaced by 200 µl of 0.5 mg/ml of 3-(4,5-dimethylthiazol-2-yl)-2,5-

diphenyl-2H-tetrazolium bromide in fresh media, and cells were incubated in the CO₂ incubator at 37°C for 2 h. Supernatants were removed from the wells, and the reduced 3-(4,5-dimethylthiazol-2-yl)-2,5-diphenyl-2H-tetrazolium bromide dye was solubilized in 200 µl/well DMSO. Absorbance at 570 nm was determined on a plate reader.

4.2.3 Flow cytometry analysis—For all the assays, cells were treated for the indicated time. To analyze the cell cycle profile, treated cells were fixed overnight with 70% EtOH at –20°C and stained with propidium iodide buffer [38 mM sodium citrate (pH 7.5), 69 µM propidium iodide, and 120 µg/mL RNase A]. Samples were mixed gently and incubated at room temperature in the dark for 15 min. Immediately before analysis by flow cytometry, 400 µL binding buffer was added to each sample. A total of 1.2×10^4 cells were acquired for each sample and a maximum of 1×10^4 cells within the gated region were analyzed.

4.2.4 *In vivo* xenograft studies—Five- to six-week-old BALB/c *nu/nu*, athymic, mice were purchased from Charles River Laboratories, Inc. (Wilmington, MA). Subconfluent HT29 cells were harvested from monolayer culture and resuspended in an equal volume of Matrigel (BD Biosciences, San Jose, CA) to a final concentration of $1 \times 10^7/0.2$ mL. At 10 weeks of age, each animal received s.c. inoculations in two sites per flank with 200 µL of HT29 cell suspension. Six animals were randomly grouped into two. Tumors were measured twice weekly with calipers, and tumor volume was calculated by the following formula: (width)²×length/2. Treatments began when the tumors reached a measurable size (~200 mm³). Treated group was intraperitoneal administrated 5 mg/kg/d of CSUOH0901 five times a week (1%DMSO, sesame oil as vehicle). The control group received the vehicle treatment. Body weights were monitored weekly as an indicator of the animals' overall health. After three weeks of treatment, the mice were euthanized and the tumors were removed, weighed.

4.2.5. Preparation of calibration standards and quality controls (QC) samples—The stock standard solutions of CSUOH0901 was prepared by dissolving in DMSO it at 1 mg/mL and stored at –20°C. One set of CSUOH0901 working solutions at 3, 10, 20, 100, 200 and 1000 ng/ml, prepared by serial diluting stock solution with 50% acetonitrile in water, was used for calibration standards. Another set of JCC76 working solutions at 3, 9, 90, and 900 ng/ml was made in the similar way and used for QC samples. All of the working solutions were freshly prepared before use. Calibration standards were prepared by spiking 5 µL different CSUOH0901 working solutions into 50 µL blank rat plasma to give the final concentration of CSUOH0901 at 0.3, 1, 2, 10, 2 and 100ng/ml. The QC samples were prepared in same way as the calibration standards at four different levels of 0.3, 0.9, 9 and 90 ng/ml, representing lower limit of quantitation (LLOQ), low QC (LQC), middle QC (MQC) and high QC (HQC) of CSUOH0901 in plasma. All of the calibration standards and QC samples were further treated in the same preparation procedure.

4.2.6. Pharmacokinetic study—Male Sprague–Dawley rats (each weight 300 – 350 g) were purchased from Charles River Laboratories International (Spencerville, OH, USA). Animals were housed in a 12 h light/dark cycle room with free access to food and water for at least 7 days to adapt the environment. All the animal experiment procedures were

performed under the guideline approved by Institutional Animal Care and Use Committee at Cleveland State University.

Before the intraperitoneal administration of CSUOH0901 at a single dose of 20 mg/kg (PBS with 0.1% Tween80, 20% DMSO as vehicle), animals were fasted overnight but with free access of water. Blood samples of 150 μ L each were collected from the saphenous veins and femoral veins into heparinized tubes at 0 hr (before drug administration) and at 0.25, 0.5, 1, 2, 4, 8 and 24h after dosing. The blood samples were centrifuged immediately at 10,000 rpm for 5 min in room temperature. The plasma samples were separated and stored at -20°C until analysis.

Plasma concentrations of CSUOH0901 were determined by a LC-MS/MS method developed and validated for this study. The LC-MS/MS method consisted of a Shimadzu HPLC system (Shimadzu, Tokyo, Japan) and an AB Sciex QTrap 5500 mass spectrometer equipped with an electrospray ionization source (ABI-Sciex, Toronto, Canada). The chromatographic separation was achieved using a C18 column (2.0 mm \times 150 mm, 5 μ m) together with 0.5 mM ammonium formate in 90% methanol for isocratic elution. The eluates were detected using multiple-reaction-monitoring (MRM) mode for CSUOH0901 (m/z 483.3 to 404.3) and the internal standard JCC76 (m/z 445 to 366.3). The liquid-liquid extraction method using the mixture of *tert*-butyl methyl ether and *n*-hexane (1:1, v/v) was optimized for plasma sample pretreatment. This analytical method was validated over the concentration range of 0.1-100 ng/mL ($r^2 = 0.999$). The intra and inter-assay variability (% coefficient of variation) and mean bias (% relative error) were evaluated and less than 15%. Plasma quantified above the highest concentration of the standard curve were diluted with blank plasma and reanalyzed.

The concentration of CSUOH0901 in rat plasma versus time profiles were analyzed to estimate pharmacokinetic parameters using WinNonlin® software version 5.2 (Pharsight Corporation, Mountain View, CA, USA). The estimated pharmacokinetic parameters including the terminal phase elimination half-life ($T_{1/2}$), and the area under the plasma concentration time curve (AUC) from time 0 to time of the last measurable concentration ($\text{AUC}_{(0-t)}$), the volume of distribution ($V_{z/F}$), the total body clearance (Cl_F), and the mean residence time (MRT) from time 0 to time of the last measurable concentration ($\text{MRT}_{(0-t)}$) were determined.

Supplementary Material

Refer to Web version on PubMed Central for supplementary material.

Acknowledgments

This research was supported by a startup fund from Cleveland State University. The research was also supported by the Translational Research Core Facility and Athymic Animal & Xenograft Core Facility of the Case Comprehensive Cancer Center (P30 CA43703). We thank the Developmental Therapeutic Program at the National Cancer Institute for screening the compound against 60 human tumor cell lines and acute toxicity studies.

References

- [1]. Williams CS, Tsujii M, Reese J, Dey SK, DuBois RN. Host cyclooxygenase-2 modulates carcinoma growth. *J. Clin. Invest.* 2000; 105:1589–1594. [PubMed: 10841517]
- [2]. Tsujii M, Kawano S, Tsuji S, Sawaoka H, Hori M, DuBois RN. Cyclooxygenase regulates angiogenesis induced by colon cancer cells. *Cell.* 1998; 93:705–716. [PubMed: 9630216]
- [3]. Tong BJ, Tan J, Tajeda L, Das SK, Chapman JA, DuBois RN, Dey SK. Heightened expression of cyclooxygenase-2 and peroxisome proliferator-activated receptor-delta in human endometrial adenocarcinoma. *Neoplasia.* 2000; 2:483–490. [PubMed: 11228540]
- [4]. Eberhart CE, Coffey RJ, Radhika A, Giardiello FM, Ferrenbach S, DuBois RN. Up-regulation of cyclooxygenase 2 gene expression in human colorectal adenomas and adenocarcinomas. *Gastroenterology.* 1994; 107:1183–1188. [PubMed: 7926468]
- [5]. Liu CH, Chang SH, Narko K, Trifan OC, Wu MT, Smith E, Haudenschild C, Lane TF, Hla T. Overexpression of cyclooxygenase-2 is sufficient to induce tumorigenesis in transgenic mice. *J. Biol. Chem.* 2001; 276:18563–18569. [PubMed: 11278747]
- [6]. Sano H, Kawahito Y, Wilder RL, Hashiramoto A, Mukai S, Asai K, Kimura S, Kato H, Kondo M, Hla T. Expression of cyclooxygenase-1 and -2 in human colorectal cancer. *Cancer Res.* 1995; 55:3785–3789. [PubMed: 7641194]
- [7]. Shattuck-Brandt RL, Varilek GW, Radhika A, Yang F, Washington MK, DuBois RN. Cyclooxygenase 2 expression is increased in the stroma of colon carcinomas from IL-10(-/-) mice. *Gastroenterology.* 2000; 118:337–345. [PubMed: 10648462]
- [8]. Rao CV, Reddy BS. NSAIDs and chemoprevention. *Curr. Cancer. Drug Targets.* 2004; 4:29–42. [PubMed: 14965265]
- [9]. Mazhar D, Gillmore R, Waxman J. COX and cancer. *QJM.* 2005; 98:711–718. [PubMed: 16170203]
- [10]. Sarkar FH, Adsule S, Li Y, Padhye S. Back to the future: COX-2 inhibitors for chemoprevention and cancer therapy. *Mini Rev. Med. Chem.* 2007; 7:599–608. [PubMed: 17584158]
- [11]. Olsen JH, Friis S, Poulsen AH, Fryzek J, Harving H, Tjonneland A, Sorensen HT, Blot W. Use of NSAIDs, smoking and lung cancer risk. *Br. J. Cancer.* 2008; 98:232–237. [PubMed: 18087276]
- [12]. Srinath P, Rao PN, Knaus EE, Suresh MR. Effect of cyclooxygenase-2 (COX-2) inhibitors on prostate cancer cell proliferation. *Anticancer Res.* 2003; 23:3923–3928. [PubMed: 14666698]
- [13]. Boland GP, Butt IS, Prasad R, Knox WF, Bundred NJ. COX-2 expression is associated with an aggressive phenotype in ductal carcinoma in situ. *Br. J. Cancer.* 2004; 90:423–429. [PubMed: 14735188]
- [14]. Keller JJ, Giardiello FM. Chemoprevention strategies using NSAIDs and COX-2 inhibitors. *Cancer. Biol. Ther.* 2003; 2:S140–9. [PubMed: 14508092]
- [15]. Dang CT, Shapiro CL, Hudis CA. Potential role of selective COX-2 inhibitors in cancer management. *Oncology (Williston Park).* 2002; 16:30–36. [PubMed: 12102578]
- [16]. Rigas B, Kashfi K. Cancer prevention: a new era beyond cyclooxygenase-2. *J. Pharmacol. Exp. Ther.* 2005; 314:1–8. [PubMed: 15805430]
- [17]. Deasy BM, O'Sullivan-Coyne G, O'Donovan TR, McKenna SL, O'Sullivan GC. Cyclooxygenase-2 inhibitors demonstrate anti-proliferative effects in oesophageal cancer cells by prostaglandin E(2)-independent mechanisms. *Cancer Lett.* 2007; 256:246–258. [PubMed: 17707579]
- [18]. Han S, Roman J. COX-2 inhibitors suppress lung cancer cell growth by inducing p21 via COX-2 independent signals. *Lung Cancer.* 2006; 51:283–296. [PubMed: 16376453]
- [19]. Hanif R, Pittas A, Feng Y, Koutsos MI, Qiao L, Staiano-Coico L, Shiff SI, Rigas B. Effects of nonsteroidal anti-inflammatory drugs on proliferation and on induction of apoptosis in colon cancer cells by a prostaglandin-independent pathway. *Biochem. Pharmacol.* 1996; 52:237–245. [PubMed: 8694848]
- [20]. Song X, Lin HP, Johnson AJ, Tseng PH, Yang YT, Kulp SK, Chen CS. Cyclooxygenase-2, player or spectator in cyclooxygenase-2 inhibitor-induced apoptosis in prostate cancer cells. *J. Natl. Cancer Inst.* 2002; 94:585–591. [PubMed: 11959891]

- [21]. Totzke G, Schulze-Osthoff K, Janicke RU. Cyclooxygenase-2 (COX-2) inhibitors sensitize tumor cells specifically to death receptor-induced apoptosis independently of COX-2 inhibition. *Oncogene*. 2003; 22:8021–8030. [PubMed: 12970750]
- [22]. Yamazaki R, Kusunoki N, Matsuzaki T, Hashimoto S, Kawai S. Selective cyclooxygenase-2 inhibitors show a differential ability to inhibit proliferation and induce apoptosis of colon adenocarcinoma cells. *FEBS Lett*. 2002; 531:278–284. [PubMed: 12417326]
- [23]. Han S, Roman J. COX-2 inhibitors suppress integrin alpha5 expression in human lung carcinoma cells through activation of Erk: involvement of Sp1 and AP-1 sites. *Int. J. Cancer*. 2005; 116:536–546. [PubMed: 15825163]
- [24]. Johnson AJ, song X, Hsu A, Chen C. Apoptosis signaling pathways mediated by cyclooxygenase-2 inhibitors in prostate cancer cells. *Adv. Enzyme Regul*. 2001; 41:221–235. [PubMed: 11384747]
- [25]. Tian G, Yu JP, Luo HS, Yu BP, Yue H, Li JY, Mei Q. Effect of nimesulide on proliferation and apoptosis of human hepatoma SMMC-7721 cells. *World J. Gastroenterol*. 2002; 8:483–487. [PubMed: 12046075]
- [26]. Tong Z, Wu X, Chen CS, Kehrer JP. Cytotoxicity of a non-cyclooxygenase-2 inhibitory derivative of celecoxib in non-small-cell lung cancer A549 cells. *Lung Cancer*. 2006; 52:117–124. [PubMed: 16497409]
- [27]. Zhu J, Huang JW, Tseng PH, Yang YT, Fowble J, Shiau CW, Shaw YJ, Kulp SK, Chen CS. From the cyclooxygenase-2 inhibitor celecoxib to a novel class of 3-phosphoinositide-dependent protein kinase-1 inhibitors. *Cancer Res*. 2004; 64:4309–4318. [PubMed: 15205346]
- [28]. Zhu J, Song X, Lin HP, Young DC, Yan S, Marquez VE, Chen CS. Using cyclooxygenase-2 inhibitors as molecular platforms to develop a new class of apoptosis-inducing agents. *J. Natl. Cancer Inst*. 2002; 94:1745–1757. [PubMed: 12464646]
- [29]. Kawamori T, Nakatsugi S, Ohta T, Sugimura T, Wakabayashi K. Chemopreventive effects of nimesulide, a selective cyclooxygenase-2 inhibitor, against PhIP-induced mammary carcinogenesis. *Adv. Exp. Med. Biol*. 2002; 507:371–376. [PubMed: 12664612]
- [30]. Nakatsugi S, Ohta T, Kawamori T, Mutoh M, Tanigawa T, Watanabe K, Sugie S, Sugimura T, Wakabayashi K. Chemoprevention by nimesulide, a selective cyclooxygenase-2 inhibitor, of 2-amino-1-methyl-6-phenylimidazo[4,5-b]pyridine (PhIP)-induced mammary gland carcinogenesis in rats. *Jpn. J. Cancer Res*. 2000; 91:886–892. [PubMed: 11011115]
- [31]. Yamamoto K, Kitayama W, Denda A, Morisaki A, Kuniyasu H, Kirita T. Inhibitory effects of selective cyclooxygenase-2 inhibitors, nimesulide and etodolac, on the development of squamous cell dysplasias and carcinomas of the tongue in rats initiated with 4-nitroquinoline 1-oxide. *Cancer Lett*. 2003; 199:121–129. [PubMed: 12969784]
- [32]. Furukawa F, Nishikawa A, Lee IS, Kanki K, Umemura T, Okazaki K, Kawamori T, Wakabayashi K, Hirose M. A cyclooxygenase-2 inhibitor, nimesulide, inhibits postinitiation phase of N-nitrosobis(2-oxopropyl)amine-induced pancreatic carcinogenesis in hamsters. *Int. J. Cancer*. 2003; 104:269–273. [PubMed: 12569549]
- [33]. Pan Y, Zhang JS, Gazi MH, Young CY. The cyclooxygenase 2-specific nonsteroidal anti-inflammatory drugs celecoxib and nimesulide inhibit androgen receptor activity via induction of c-Jun in prostate cancer cells. *Cancer Epidemiol. Biomarkers Prev*. 2003; 12:769–774. [PubMed: 12917209]
- [34]. Li JY, Wang XZ, Chen FL, Yu JP, Luo HS. Nimesulide inhibits proliferation via induction of apoptosis and cell cycle arrest in human gastric adenocarcinoma cell line. *World J. Gastroenterol*. 2003; 9:915–920. [PubMed: 12717830]
- [35]. Liang M, Yang H, Fu J. Nimesulide inhibits IFN-gamma-induced programmed death-1-ligand 1 surface expression in breast cancer cells by COX-2 and PGE2 independent mechanisms. *Cancer Lett*. 2009; 276:47–52. [PubMed: 19046800]
- [36]. Nam KT, Hahm KB, Oh SY, Yeo M, Han SU, Ahn B, Kim YB, Kang JS, Jang DD, Yang KH, Kim DY. The selective cyclooxygenase-2 inhibitor nimesulide prevents Helicobacter pylori-associated gastric cancer development in a mouse model. *Clin. Cancer Res*. 2004; 10:8105–8113. [PubMed: 15585646]

- [37]. Hida T, Kozaki K, Muramatsu H, Masuda A, Shimizu S, Mitsudomi T, Sugiura T, Ogawa M, Takahashi T. Cyclooxygenase-2 inhibitor induces apoptosis and enhances cytotoxicity of various anticancer agents in non-small cell lung cancer cell lines. *Clin. Cancer Res.* 2000; 6:2006–2011. [PubMed: 10815926]
- [38]. Eibl G, Reber HA, Wentz MN, Hines OJ. The selective cyclooxygenase-2 inhibitor nimesulide induces apoptosis in pancreatic cancer cells independent of COX-2. *Pancreas.* 2003; 26:33–41. [PubMed: 12499915]
- [39]. Chen B, Su B, Chen S. A COX-2 inhibitor nimesulide analog selectively induces apoptosis in Her2 overexpressing breast cancer cells via cytochrome c dependent mechanisms. *Biochem. Pharmacol.* 2009; 77:1787–1794. [PubMed: 19428334]
- [40]. Zhong B, Cai X, Yi X, Zhou A, Chen S, Su B. *In vitro* and *in vivo* effects of a cyclooxygenase-2 inhibitor nimesulide analog JCC76 in aromatase inhibitors-insensitive breast cancer cells. *J. Steroid Biochem. Mol. Biol.* 2011; 126:10–18. [PubMed: 21458568]
- [41]. Su B, Darby MV, Brueggemeier RW. Synthesis and biological evaluation of novel sulfonanilide compounds as antiproliferative agents for breast cancer. *J. Comb. Chem.* 2008; 10:475–483. [PubMed: 18380483]
- [42]. Su B, Diaz-Cruz ES, Landini S, Brueggemeier RW. Novel sulfonanilide analogues suppress aromatase expression and activity in breast cancer cells independent of COX-2 inhibition. *J. Med. Chem.* 2006; 49:1413–1419. [PubMed: 16480277]
- [43]. Renard JF, Julemont F, de Leval X, Pirotte B. The use of nimesulide and its analogues in cancer chemoprevention. *Anticancer Agents Med. Chem.* 2006; 6:233–237. [PubMed: 16712451]
- [44]. Julemont F, de Leval X, Michaux C, Damas J, Charlier C, Durant F, Pirotte B, Dogne JM. Spectral and crystallographic study of pyridinic analogues of nimesulide: determination of the active form of methanesulfonamides as COX-2 selective inhibitors. *J. Med. Chem.* 2002; 45:5182–5185. [PubMed: 12408728]
- [45]. Boelsterli UA, Ho HK, Zhou S, Leow KY. Bioactivation and hepatotoxicity of nitroaromatic drugs. *Curr. Drug Metab.* 2006; 7:715–727. [PubMed: 17073576]
- [46]. Su B, Chen S. Lead optimization of COX-2 inhibitor nimesulide analogs to overcome aromatase inhibitor resistance in breast cancer cells. *Bioorg. Med. Chem. Lett.* 2009; 19:6733–6735. [PubMed: 19854050]
- [47]. Sparreboom A, van Tellingen O, Nooijen WJ, Beijnen JH. Nonlinear pharmacokinetics of paclitaxel in mice results from the pharmaceutical vehicle Cremophor EL. *Cancer Res.* 1996; 56:2112–2115. [PubMed: 8616858]

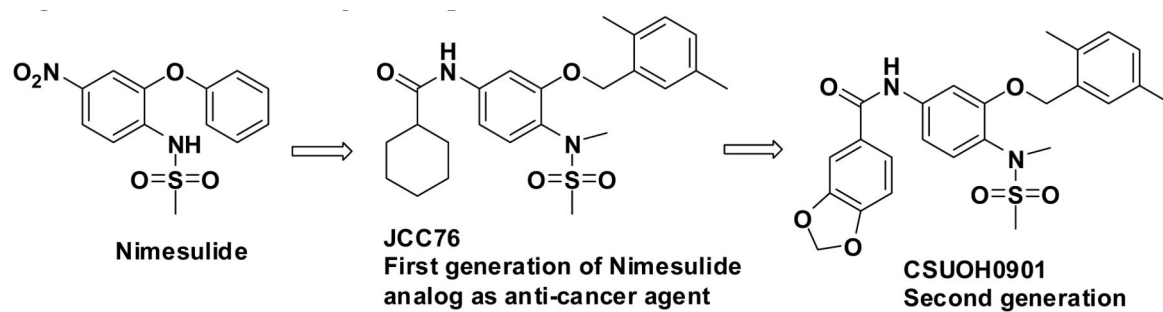


Figure 1.
Anti-cancer drug development based on COX-2 inhibitor nimesulide

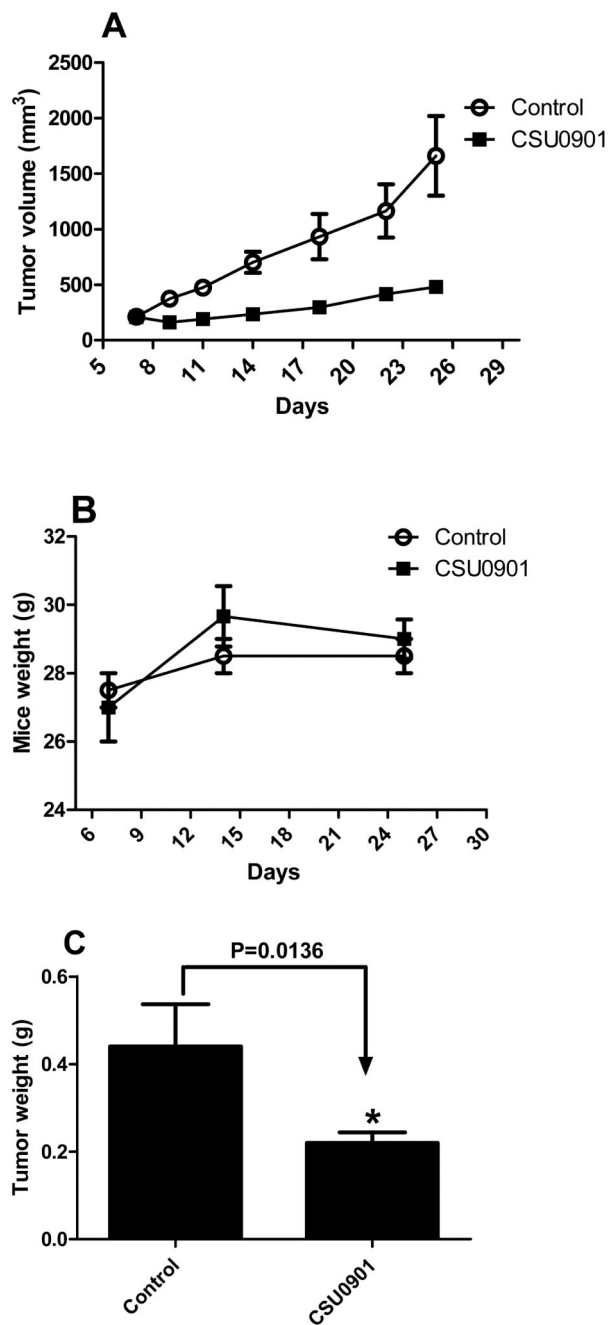


Figure 2.

In vivo anti-cancer evaluation of CSUOH0901. A. Nude mice bearing HT29 xenograft after the treatment. The treatment group is significantly smaller than the control group (n=6); B Mice weight changing (n=3); C HT29 tumor weight comparison (n=6). * $P < 0.05$ vs control

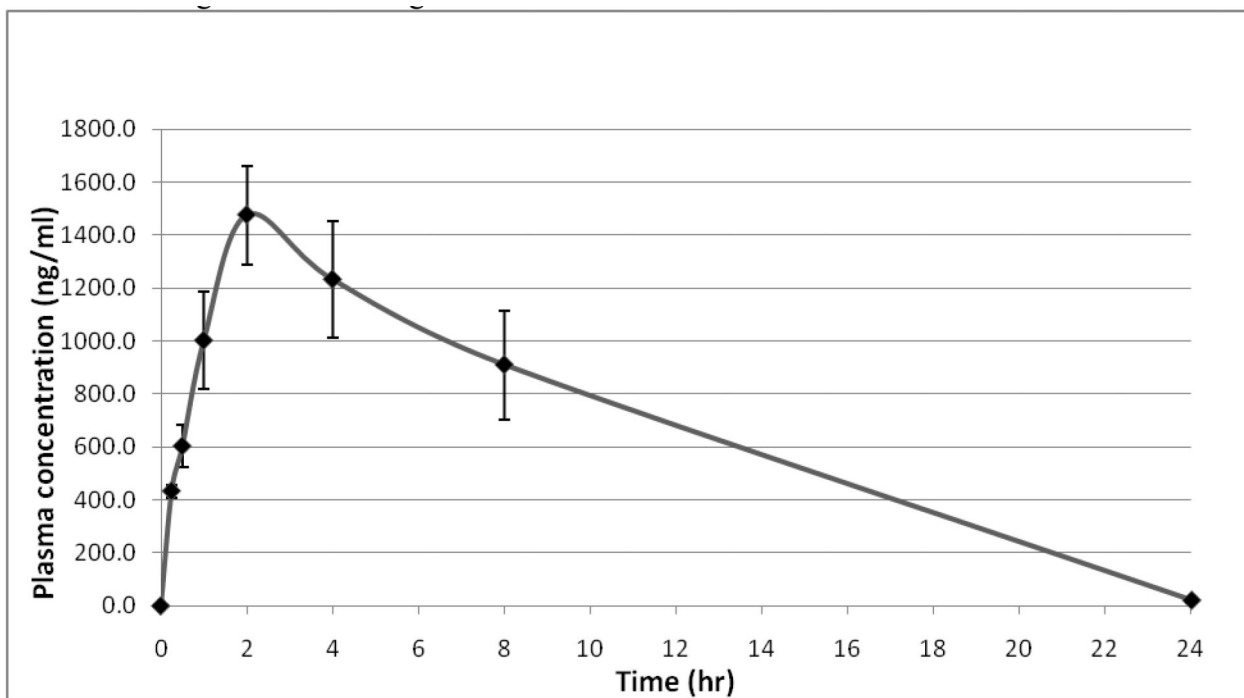
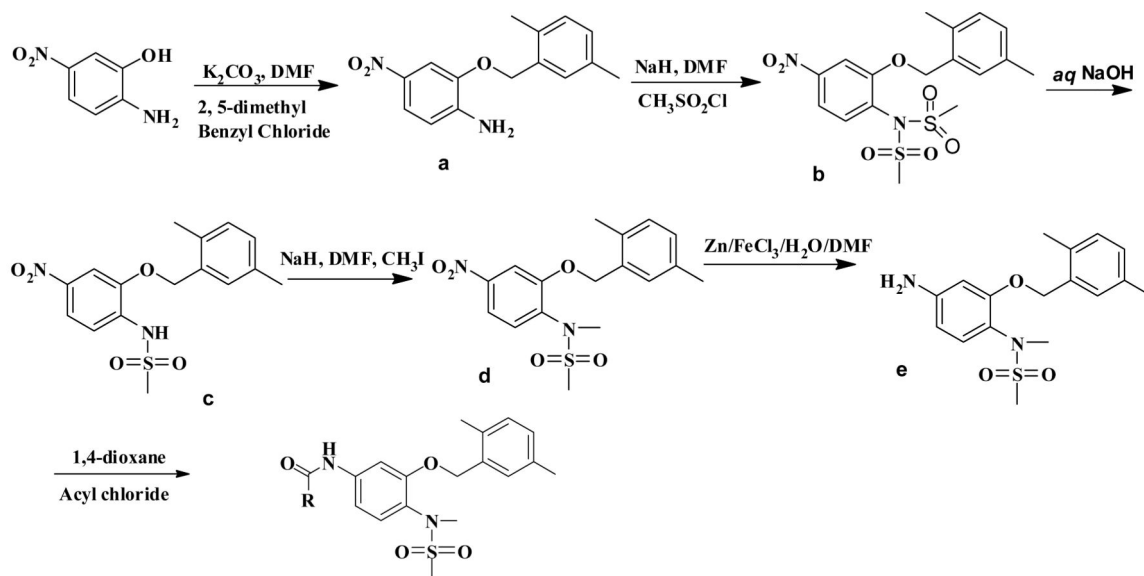


Figure 3. CSUOH0901 rats blood concentrations vs time. CSUOH0901 was administrated to rats (n=3) intraperitoneally with 20mg/kg. Blood samples of 150 μ L each were collected from the saphenous veins and femoral veins into heparized tubes at 0 hr (before drug administration) and at 0.25, 0.5, 1, 2, 4, 8 and 24h after dosing. The blood drug concentration was then determined with LC-MS/MS.

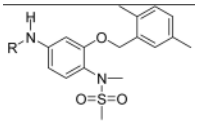
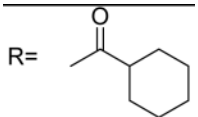
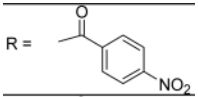
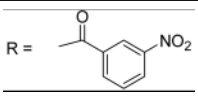
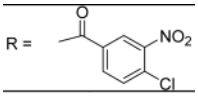
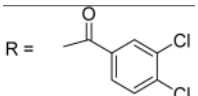
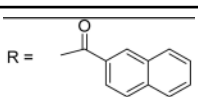
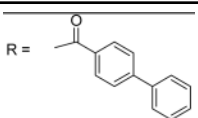
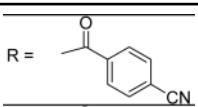
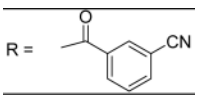
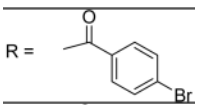


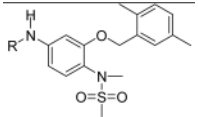
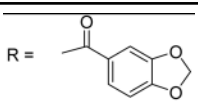
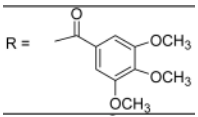
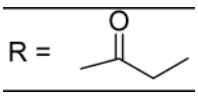
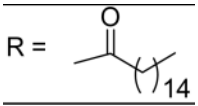
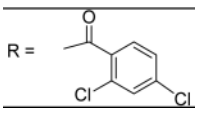
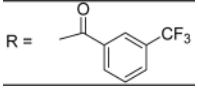
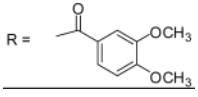
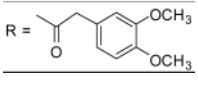
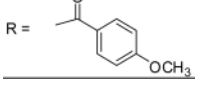
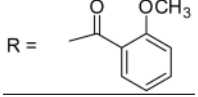
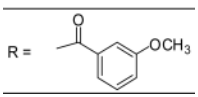
- | | |
|--------------------------------------|---|
| 1 R= 4-Nitro-phenyl (88%) | 20 R= 3-Methoxy-phenyl (91%) |
| 2 R= 3-Nitro-phenyl (86%) | 21 R= 3-Methoxy-2,4,5-trifluorophenyl (98%) |
| 3 R= 4-Chloro-3-nitro-phenyl (82%) | 22 R= 3-Pentyl (96%) |
| 4 R= 3,4-Dichloro-phenyl (69%) | 23 R= Cyclopentyl (93%) |
| 5 R= 2-Naphthyl (72%) | 24 R= Benzyl (99%) |
| 6 R= 4-Biphenyl (73%) | 25 R= 1-Naphthyl (83%) |
| 7 R= 4-Cyano-phenyl (75%) | 26 R= 3,5-Bis(trifluoromethyl)-phenyl (93%) |
| 8 R= 3-Cyano-phenyl (71%) | 27 R= 3-Bromophenyl (99%) |
| 9 R= 4-Bromo-phenyl (80%) | 28 R= 4-Chlorophenyl (99%) |
| 10 R= 5-Benzo[1,3]dioxolyl(71%) | 29 R= 4-Iodophenyl (96%) |
| 11 R= 3,4,5-Trimethoxy-phenyl (93%) | 30 R= 4-Methylsulfonyl-phenyl (92%) |
| 12 R= Propionyl (88%) | 31 R= 4-Dimethylamino-phenyl (66%) |
| 13 R= Hexadecanyl (98%) | 32 R= 4-Ethoxy-phenyl (70%) |
| 14 R= 2,4-Dichloro-phenyl (80%) | 33 R= 4-Ethyl-phenyl (64%) |
| 15 R= 3-Trifluoromethyl-phenyl (93%) | 34 R= 4-Trifluoromethyl-phenyl (84%) |
| 16 R= 3,4-Dimethoxy-phenyl (93%) | 35 R= 4-Trifluoromethoxy-phenyl(79%) |
| 17 R= 3,4-Dimethoxy-benzyl (95%) | 36 R= 4-Methyl-phenyl (69%) |
| 18 R= 4-Methoxy-phenyl (96%) | 37 R= 2-Furyl (66%) |
| 19 R= 2-Methoxy-phenyl (97%) | 38 R= 2-Thiophenyl (72%) |
| | 39 R= 5-Isoxazolyl(99%) |

Scheme 1.
Synthesis of JCC76 analogs

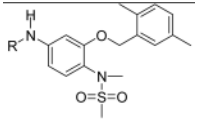
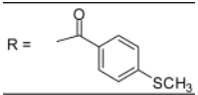
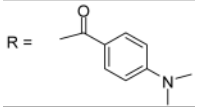
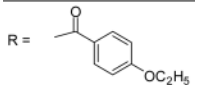
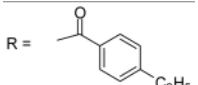
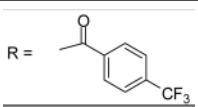
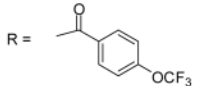
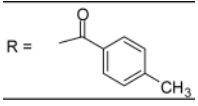
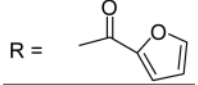
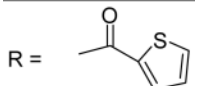
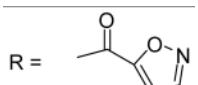
Table 1

Inhibition of cancer cell growth of the JCC76 analogs

Entry		IC ₅₀ against SKBR-3 breast cancer cell growth
JCC76		1.38±0.10 μM
1		1.13±0.10 μM
2		1.97±0.21 μM
3		3.35±0.40 μM
4		0.91±0.05 μM
5		0.21±0.01 μM
6		2.28±0.09 μM
7		1.46±0.06 μM
8		3.01±0.12 μM
9		0.22±0.01 μM

Entry		IC ₅₀ against SKBR-3 breast cancer cell growth
10 (CSUOH0901; NSC751382)	R = 	0.20±0.01 μM
11	R = 	0.30±0.02 μM
12	R = 	43.27±7.38 μM
13	R = 	11.05±4.76 μM
14	R = 	0.80±0.01 μM
15	R = 	2.78±0.29 μM
16	R = 	0.19±0.14 μM
17	R = 	34.02±2.01 μM
18	R = 	0.15±0.05 μM
19	R = 	0.68±0.32 μM
20	R = 	6.88±3.18 μM

Entry		IC ₅₀ against SKBR-3 breast cancer cell growth
21		2.16±1.08 μM
22		51.24±4.49 μM
23		11.21±4.47 μM
24		>100 μM
25		3.95±2.09 μM
26		55.35±4.11 μM
27		7.34±3.99 μM
28		2.15±0.94 μM
29		0.13±0.07 μM

Entry		IC ₅₀ against SKBR-3 breast cancer cell growth
30	R = 	0.66±0.32 μM
31	R = 	1.01±0.52 μM
32	R = 	0.41±0.03 μM
33	R = 	2.48±1.44 μM
34	R = 	1.20±0.59 μM
35	R = 	0.58±0.29 μM
36	R = 	2.82±1.51 μM
37	R = 	16.65±2.26 μM
38	R = 	20.12±5.28 μM
39	R = 	21.88±5.08 μM

Cells were treated with indicated compounds at various concentrations by six replicates for 48h and cell viability was measured by MTT assay as described in the experimental section.

Table 2
Summary of altered cell cycle distribution in response to treatment with CSUOH0901(NSC751382)

SKBR-3 cells were treated for different time period with the indicated concentrations of compound. Cells were processed for FACS using propidium iodide staining as described. Percent distribution of cells in each cell cycle phase was displayed.

Time	Concentrations of CSUOH0901	Sub-G1 %	G1 %	S %	G2/M %
3h	0.10(μ M)	3.12	70.84	17.20	8.83
	0.25(μ M)	3.23	69.63	16.34	10.77
	0.50(μ M)	3.43	67.14	17.76	11.54
	5.0(μ M)	2.81	69.09	16.49	11.57
6h	0.10(μ M)	3.60	71.43	15.84	9.07
	0.25(μ M)	3.49	72.21	14.95	9.32
	0.50(μ M)	4.03	67.10	14.73	13.90
	5.0(μ M)	3.42	64.76	14.61	17.19
12h	0.10(μ M)	5.27	73.14	8.17	12.05
	0.25(μ M)	6.85	73.62	6.14	13.35
	0.50(μ M)	6.36	63.15	5.94	24.26
	5.0(μ M)	9.76	63.71	5.99	20.54
18h	0.10(μ M)	6.04	75.43	8.71	9.71
	0.25(μ M)	8.89	73.42	6.81	10.57
	0.50(μ M)	8.47	61.19	7.28	22.27
	5.0(μ M)	8.31	63.55	6.73	21.80
24h	0.10(μ M)	11.78	67.90	8.91	11.23
	0.25(μ M)	24.95	41.27	10.87	22.53
	0.50(μ M)	27.94	31.77	11.21	28.14
	5.0(μ M)	27.62	31.87	11.53	28.29

Table 3

Growth inhibitory effect of CSUOH0901 on 60 human tumor cell lines. Growth inhibition of 50 % (GI50), total growth inhibition (TGI), and LC50 are listed in the table.

Panel/Cell Line	GI50	TGI	LC50
Leukemia			
CCRF-CEM	4.85E-8	> 1.00E-4	> 1.00E-4
HL-60(TB)	2.69E-8	9.67E-8	> 1.00E-4
K-562	4.03E-8	> 1.00E-4	> 1.00E-4
MOLT-4	1.63E-7	> 1.00E-4	> 1.00E-4
RPMI-8226	2.90E-7		> 1.00E-4
Non-Small Cell Lung Cancer			
A549/ATCC	2.78E-7	1.36E-5	> 1.00E-4
EKVX	5.98E-7	> 1.00E-4	> 1.00E-4
HOP-62	3.29E-7	> 1.00E-4	> 1.00E-4
HOP-92	3.22E-6	> 1.00E-4	> 1.00E-4
NCI-H226	6.86E-7	> 1.00E-4	> 1.00E-4
NCI-H23	1.62E-7	> 1.00E-4	> 1.00E-4
NCI-H322M	4.68E-7	> 1.00E-4	> 1.00E-4
NCI-H460	1.84E-7	7.44E-7	> 1.00E-4
NCI-H522	3.35E-8	2.40E-7	> 1.00E-4
Colon Cancer			
COLO 205	3.18E-7	1.07E-6	> 1.00E-4
HCC-2998	1.20E-7	3.92E-7	2.97E-6
HCT-116	7.53E-8	1.02E-6	> 1.00E-4
HCT-15	2.89E-7	> 1.00E-4	> 1.00E-4
HT29	7.72E-8	4.19E-7	> 1.00E-4
KM12	8.55E-8	1.13E-6	> 1.00E-4
SW-620	1.12E-7	> 1.00E-4	> 1.00E-4
CNS Cancer			
SF-268	2.88E-7	> 1.00E-4	> 1.00E-4
SF295	9.83E-8	6.26E-7	> 1.00E-4
SF539	1.25E-7		> 1.00E-4
SNB-19	5.37E-7	> 1.00E-4	> 1.00E-4
SNB-75	2.66E-7		> 1.00E-4
U251	2.66E-7	2.19E-5	> 1.00E-4
Melanoma			
LOXIMVI	6.66E-8	> 1.00E-4	> 1.00E-4
MALME-3M	2.29E-7	> 1.00E-4	> 1.00E-4
M14	7.57E-8	6.69E-7	> 1.00E-4
MDA-MB-435	2.85E-8	9.14E-8	> 1.00E-4
SK-MEL-2	8.97E-8	6.16E-7	> 1.00E-4
SK-MEL-28	6.92E-7	> 1.00E-4	> 1.00E-4

Panel/Cell Line	GI50	TGI	LC50
SK-MEL-5	2.53E-7	1.65E-6	3.41E-5
UACC-257	1.44E-7	> 1.00E-4	> 1.00E-4
UACC-62	4.14E-7	> 1.00E-4	> 1.00E-4
Ovarian Cancer			
IGROV1	2.37E-7	> 1.00E-4	> 1.00E-4
OVCAR-3	3.96E-8	1.66E-7	
OVCAR-4		> 1.00E-4	> 1.00E-4
OVCAR-5	5.38E-7	> 1.00E-4	> 1.00E-4
OVCAR-8	2.65E-7	> 1.00E-4	> 1.00E-4
NCI/ADR-RES	5.62E-8	4.07E-7	> 1.00E-4
SK-OV-3	2.85E-7	> 1.00E-4	> 1.00E-4
Renal Cancer			
786-0	1.91E-7	1.11E-6	> 1.00E-4
A498	1.22 E-7	8.53E-7	> 1.00E-4
ACHN	6.87 E-7	> 1.00E-4	> 1.00E-4
CAKI-1	1.26 E-7	> 1.00E-4	> 1.00E-4
RXF 393	1.28 E-7	4.03E-7	> 1.00E-4
SN12C	4.72 E-7	> 1.00E-4	> 1.00E-4
TK-10	3.54 E-7	> 1.00E-4	> 1.00E-4
UO-31	3.95 E-7	> 1.00E-4	> 1.00E-4
Prostate Cancer			
PC-3	6.77E-8	> 1.00E-4	> 1.00E-4
DU-145	1.59E-7	4.57E-7	> 1.00E-4
Breast Cancer			
MCF7	1.20E-7	> 1.00E-4	> 1.00E-4
MDA-MB-231/ATCC	2.56E-7	9.26E-7	> 1.00E-4
HS 578T	8.70E-8		> 1.00E-4
BT-549	6.56E-7	> 1.00E-4	> 1.00E-4
T-47D	6.82E-7	> 1.00E-4	> 1.00E-4
MDA-MB-468	1.55E-7	4.01E-7	1.99E-5

Table 4

The pharmacokinetic parameters of CSUOH0901

Parameters	Rat 1	Rat 2	Rat 3	Mean	S.D.
$T_{1/2}$ (h)	2.44	3.71	3.21	3.12	0.64
$AUC_{(0-t)}$ (ng*h/mL)	16466	22648	9718	16277	6467
$V_{z/F}$ (L/kg)	1.51	1.65	3.33	2.16	1.01
Cl/f (L/h)	0.42	0.32	0.70	0.48	0.20
$MRT_{(0-t)}$ (h)	5.95	6.43	5.62	6.00	0.40